

**Ideas about a pitch control mechanism for the 2-bladed rotor of the VIRYA-5 windmill ( $\lambda_d = 7$ , Gö 711 airfoil) meant for connection to a 34-pole PM-generator for driving an asynchronous motor of a centrifugal pump. Description of the 34-pole generator.**

ing. A. Kragten

December 2016

reviewed December 2024 (chapter 9.8 added)

KD 622

It is allowed to copy this report for private use. It is allowed to use the principles of the described pitch control mechanism, the rotor and the generator. The windmill and the generator are not yet tested.

Engineering office Kragten Design  
Populierenlaan 51  
5492 SG Sint-Oedenrode  
The Netherlands  
telephone: +31 413 475770  
e-mail: [info@kdwindturbines.nl](mailto:info@kdwindturbines.nl)  
website: [www.kdwindturbines.nl](http://www.kdwindturbines.nl)

Contains	page
1 Introduction	3
2 Description of the rotor of the VIRYA-5 windmill	4
3 Calculations of the rotor geometry	4
4 Determination of the $C_p$ - $\lambda$ and the $C_q$ - $\lambda$ curves	5
5 Determination of the P-n curves, the optimum cubic line and the lines for constant f	7
6 Description of the 34-pole PM-generator	10
7 Checking if a 3-phase current is generated	13
8 Calculation of the flux density in the air gap and the stator spokes	15
9 Description of the pitch control mechanism	16
9.1 General aspects of pitch control systems	16
9.2 Choices made for the pitch control system of the VIRYA-5	18
9.3 Determination of the aerodynamic moment and the spring force	20
9.4 Determination of the friction moment for the Permaglide bearings	23
9.5 Checking of the load on the thrust ball bearings	24
9.6 Increase of $M_h$ by choosing the blade axis closer to the nose	25
9.7 Determination of the compression spring geometry	27
9.8 Effect of braking the rotor on the safety system	29
10 Description of the vane	30
11 References	31

## 1 Introduction

The VIRYA-5 windmill has a 2-bladed rotor with wooden blades and a 34-pole PM-generator meant for connection to the asynchronous motor of a centrifugal pump. The first version of the VIRYA-5 windmill is described in report KD 614 (ref. 1). For this first version, the windmill was equipped with the hinged side vane safety system which is used in all other VIRYA windmills. This safety system works fine if the windmill is used for battery charging. But it might be that the rotational speed isn't limited sharp enough for use with a 34-pole PM-generator and the asynchronous motor of a centrifugal pump. It might be that the maximum frequency which may happen is larger than that what is allowable for the pump motor and the centrifugal pump.

The reason is that the hinged side vane safety system is steered by the rotor thrust and so the thrust is limited very well. However, the maximal rotational speed for high wind speeds depends on the load of the generator. In KD 614 it is assumed that a 1.1 kW pump loaded at a factor 0.8 of its nominal power, gives a load which is that strong that the working point of the generator is lying about at the optimum cubic line of the rotor. But there are situations where a 1.1 kW motor is supplying much less power, for instance when the water level in the well has risen. For this situation, the maximum frequency of the generator may become too high. This problem can be solved if a safety system is used which is directly steered by the rotational speed. Such safety system makes use of variation of the blade angle of the blades and it is also called a pitch control safety system.

A pitch control mechanism has already been described in report KD 437 (ref. 2) for the rotor of VIRYA-15 windmill. Although the rotor of the VIRYA-15 has only two blades, the pitch control mechanism is still rather complicated. This is caused by the fact that the movement of the blades is coupled by a mechanism with a central bush and a central spring. It seems possible to design a good working pitch control mechanism for the VIRYA-5 rotor with for which the movement of both blades is not connected and this system will therefore be much simpler. This pitch control system is described in chapter 9. As the main interest for the VIRYA-5 is expected in developing countries, the pitch control mechanism must be as simple as possible.

The VIRYA-5 makes use of a 34-pole PM-generator. The generator is made from the housing of a 6-pole, 5.5 kW asynchronous motor frame size 132 with stator lamination of manufacture Kienle & Spiess. The 34-pole generator is described in detail in chapter 6.

The tower is identical to the 12 m tower of the VIRYA-4.6B2. As an alternative, a shorter tower can be used which is built up from two tubular sections. The lower section will be made of 6 m, 5" gas pipe. The upper section will be made of 3 m, 3" gas pipe. The overlap in between both sections will be about 0.4 m, so the total tower height will be about 8.6 m. This tower is described in report KD 582 (ref. 3) for the VIRYA-4.6B2.

In stead of direct coupling to the motor of a centrifugal pump, the windmill can also be used for battery charging if the generator is provided with a low voltage winding and if the winding is rectified in star. Rectification of the winding is described in report KD 340 (ref. 4).

The rotor calculations and the description of the 34-pole generator as given in report KD 614 are also given in this new report KD 622 which makes that KD 614 isn't needed to understand KD 622.

## 2 Description of the rotor of the VIRYA-5 windmill

The 2-bladed rotor of the VIRYA-5 windmill has a diameter  $D = 5$  m and a design tip speed ratio  $\lambda_d = 7$ . Advantages of a 2-bladed rotor are that no welded spoke assembly is required, that the rotor can be balanced easily and that it can be transported completely mounted. A disadvantage is that the gyroscopic moment in the rotor shaft is fluctuating. This problem is minimised because a double vane is used which gives the head a large moment of inertia and the head will therefore move slowly at variations of the wind direction (see chapter 10).

The rotor has blades with a constant chord and no twist and is provided with a Gö 711 airfoil which is flat over 97.5 % of the chord. The aerodynamic characteristics of this airfoil are described in report KD 285 (ref. 5). A blade is made out of a wooden plank with dimensions of  $36 * 240 * 2350$  mm. The Gö 711 airfoil is made over the outer 2000 mm. The inner 350 mm has a flat part at the back side for connection of the blade to the pitch control mechanism. The blades are connected to each other by a 1000 mm long connecting strip with a width of 50 mm and a thickness of 25 mm. This strip is much stiffer than the strip size  $120 * 10$  mm described in KD 614. This much stiffer strip prevents clamping of the blade shaft bearings by bending of the strip because of the blade load. The strip is also much stronger, so chapter 6 in KD 614 about calculation of the strength of the strip is cancelled. Details of the pitch control mechanism are given in chapter 9.

The central strip is bolted to the hub by means of two bolts M16. The hub is made from two halves which are bolted together and therefore the hub can always be removed, even if the shaft is rusted. The rotor is balanced by adding balance weights under the connecting bolts. A sketch of the VIRYA-5 rotor is given in figure 1.

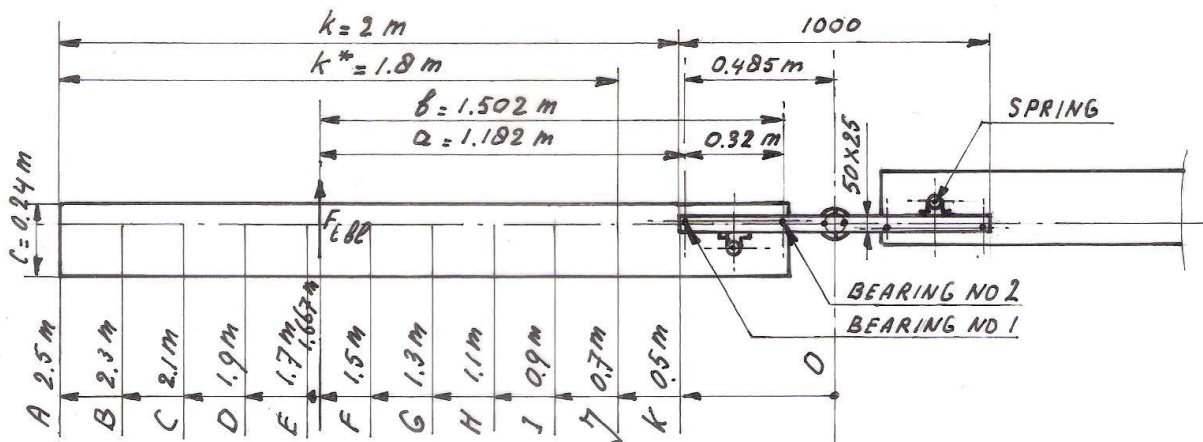


fig. 1 Sketch VIRYA-5 rotor

## 3 Calculation of the rotor geometry

The rotor geometry is determined using the method and the formulas as given in report KD 35 (ref. 6). This report (KD 622) has its own formula numbering. Substitution of  $\lambda_d = 7$  and  $R = 2.5$  m in formula (5.1) of KD 35 gives:

$$\lambda_{r,d} = 2.8 * r \quad (-) \quad (1)$$

Formula's (5.2) and (5.3) of KD 35 stay the same so:

$$\beta = \phi - \alpha \quad (^\circ) \quad (2)$$

$$\phi = 2/3 \arctan 1 / \lambda_{r,d} \quad (^\circ) \quad (3)$$

Substitution of  $B = 2$  and  $c = 0.24$  m in formula (5.4) of KD 35 gives:

$$C_1 = 52.360 r (1 - \cos\phi) \quad (-) \quad (4)$$

Substitution of  $V = 5$  m/s and  $c = 0.24$  m in formula (5.5) of KD 35 gives:

$$Re_r = 0.8 * 10^5 * \sqrt{(\lambda_{rd}^2 + 4/9)} \quad (-) \quad (5)$$

The blade is calculated for eleven stations A till K which have a distance of 0.2 m of one to another. Five more stations are chosen than in report KD 614 because this appears to be easy for the calculation of the aerodynamic pitch moment. Cross section K corresponds to the end of the connecting strip. The blade has a constant chord and the calculations therefore correspond with the example as given in chapter 5.4.2 of KD 35. This means that the blade is designed with a low lift coefficient at the tip and with a high lift coefficient at the root. First the theoretical values are determined for  $C_1$ ,  $\alpha$  and  $\beta$  and next  $\beta$  is linearised such that the twist is constant and that the linearised values for the outer part of the blade correspond as good as possible with the theoretical values. The result of the calculations is given in table 1.

The aerodynamic characteristics of the Gö 711 airfoil are given in report KD 285 (ref. 5). This airfoil has only be measured for  $Re = 4 * 10^5$  but the VIRYA-5 rotor is rather big and the design tip speed ratio is rather high and the calculated local Reynolds numbers for the most important outer blade sections are therefore rather high.

station	r (m)	$\lambda_{rd}$ (-)	$\phi$ (°)	c (m)	$C_{1th}$ (-)	$C_{1lin}$ (-)	$Re_r * 10^{-5}$ V = 5 m/s	$Re * 10^{-5}$ Gö 711	$\alpha_{th}$ (°)	$\alpha_{lin}$ (°)	$\beta_{th}$ (°)	$\beta_{lin}$ (°)	$C_d/C_{1lin}$ (-)
A	2.5	7	5.4	0.24	0.59	0.62	5.63	4	-1	-0.6	6.4	6.0	0.022
B	2.3	6.44	5.9	0.24	0.63	0.65	5.18	4	-0.4	-0.1	6.3	6.0	0.021
C	2.1	5.88	6.4	0.24	0.69	0.70	4.73	4	0.2	0.4	6.2	6.0	0.020
D	1.9	5.32	7.1	0.24	0.76	0.76	4.29	4	1.1	1.1	6.0	6.0	0.017
E	1.7	4.76	7.9	0.24	0.85	0.82	3.85	4	2.1	1.9	5.8	6.0	0.016
F	1.5	4.2	8.9	0.24	0.95	0.91	3.40	4	3.4	2.9	5.5	6.0	0.015
G	1.3	3.64	10.2	0.24	1.08	1.01	2.96	4	5.2	4.2	5.0	6.0	0.015
H	1.1	3.08	12.0	0.24	1.26	1.14	2.52	4	7.5	6.0	4.5	6.0	0.019
I	0.9	2.52	14.4	0.24	1.49	1.34	2.09	4	11.5	8.4	2.5	6.0	0.021
J	0.7	1.96	18.0	0.24	1.80	1.49	1.66	4	-	12.0	-	6.0	0.040
K	0.5	1.4	23.7	0.24	2.21	1.36	1.24	4	-	17.7	-	6.0	0.145

table 1 Calculation of the blade geometry of the VIRYA-5 rotor

No value for  $\alpha_{th}$  and therefore for  $\beta_{th}$  is found for stations J and K because the required  $C_1$  values can't be generated. The variation of the theoretical blade angle  $\beta_{th}$  is only little for the most important outer stations A up to G and varies in between  $6.4^\circ$  and  $5.0^\circ$ . Therefore it is allowed to take a constant value of  $6^\circ$  for the whole blade. So the blade has no twist.

#### 4 Determination of the $C_p$ - $\lambda$ and the $C_q$ - $\lambda$ curves

The determination of the  $C_p$ - $\lambda$  and  $C_q$ - $\lambda$  curves is given in chapter 6 of KD 35. The average  $C_d/C_1$  ratio for the most important outer part of the blade is about 0.02. Figure 4.6 of KD 35 (for  $B = 2$ ) and  $\lambda_{opt} = 7$  and  $C_d/C_1 = 0.02$  gives  $C_{p th} = 0.46$ .

The blade is stalling in between station J and K. For the calculation of the maximum  $C_p$  therefore not the blade length  $k = 2$  m for which the blade has an airfoil, is taken into account but only the part up to station J. This gives an effective blade length  $k' = 1.8$  m.

Substitution of  $C_{p th} = 0.46$ ,  $R = 2.5$  m and effective blade length  $k' = 1.8$  m in formula 6.3 of KD 35 gives  $C_{p max} = 0.42$ .  $C_{q opt} = C_{p max} / \lambda_{opt} = 0.42 / 7 = 0.06$ .

Substitution of  $\lambda_{opt} = \lambda_d = 7$  in formula 6.4 of KD 35 gives  $\lambda_{unl} = 11.2$ . The starting torque coefficient is calculated with formula 6.12 of KD 35 which is given by:

$$C_{q\ start} = 0.75 * B * (R - \frac{1}{2}k) * C_1 * c * k / \pi R^3 \quad (-) \quad (6)$$

The blade angle is  $6^\circ$  for the whole blade. For a non rotating rotor, the angle of attack  $\alpha$  is therefore  $90^\circ - 6^\circ = 84^\circ$ . The aerodynamic characteristics for the Gö 711 aren't given for large angles of  $\alpha$ . However, it is assumed that the characteristics of the Gö 623 airfoil can be used for large angles of  $\alpha$ . The estimated  $C_l$ - $\alpha$  curve for large values of  $\alpha$  is given as figure 5.10 of KD 35 (ref. 6). For  $\alpha = 84^\circ$  it can be read that  $C_l = 0.21$ . The whole blade is stalling during starting and therefore now the part of the blade which is provided with an airfoil, so the blade length outside the connecting strip which has a length  $k = 2$  m, is taken into account.

Substitution of  $B = 2$ ,  $R = 2.5$  m,  $k = 2$  m,  $C_l = 0.21$  and  $c = 0.24$  m in formula 6 gives that  $C_{q\ start} = 0.0046$ . For the ratio between the starting torque and the optimum torque we find that it is  $0.0046 / 0.06 = 0.077$ . This is acceptable for a rotor with  $\lambda_d = 7$ .

The starting wind speed  $V_{start}$  of the rotor is calculated with formula 8.6 of KD 35 which is given by:

$$V_{start} = \sqrt{\left( \frac{Q_s}{C_{q\ start} * \frac{1}{2}\rho * \pi R^3} \right)} \quad (\text{m/s}) \quad (7)$$

The 34-pole generator has not yet been built so the sticking torque has not yet been measured. The sticking torque of the VIRYA-4.6 generator  $Q_s$  has been measured at stand still position and it is 1.6 Nm. Assume that the sticking torque of the VIRYA-5 generator is 2 Nm.

Substitution of  $Q_s = 2$  Nm,  $C_{q\ start} = 0.0046$ ,  $\rho = 1.2$  kg/m<sup>3</sup> and  $R = 2.5$  m in formula 7 gives that  $V_{start} = 3.8$  m/s. This is acceptable low for a 2-bladed rotor with a design tip speed ratio of 7.

In chapter 6.4 of KD 35 it is explained how rather accurate  $C_p$ - $\lambda$  and  $C_q$ - $\lambda$  curves can be determined if only two points of the  $C_p$ - $\lambda$  curve and one point of the  $C_q$ - $\lambda$  curve are known. The first part of the  $C_q$ - $\lambda$  curve is determined according to KD 35 by drawing an S-shaped line which is horizontal for  $\lambda = 0$ . Kragten Design developed a method with which the value of  $C_q$  for low values of  $\lambda$  can be determined (see report KD 97 ref. 7). With this method, it can be determined that the  $C_q$ - $\lambda$  curve is about straight and horizontal for low values of  $\lambda$  if a Gö 623 or a Gö 711 airfoil is used. A scale model of a three bladed rotor with constant chord and blade angle and with a design tip speed ratio  $\lambda_d = 6$  has been measured in the wind tunnel already on 20-11-1980. It has been found that the maximum  $C_p$  was more than 0.4 and that the  $C_q$ - $\lambda$  curve for low values of  $\lambda$  was not horizontal but somewhat rising. This effect has been taken into account and the estimated  $C_p$ - $\lambda$  and  $C_q$ - $\lambda$  curves for the VIRYA-5 rotor are given in figure 2 and 3.

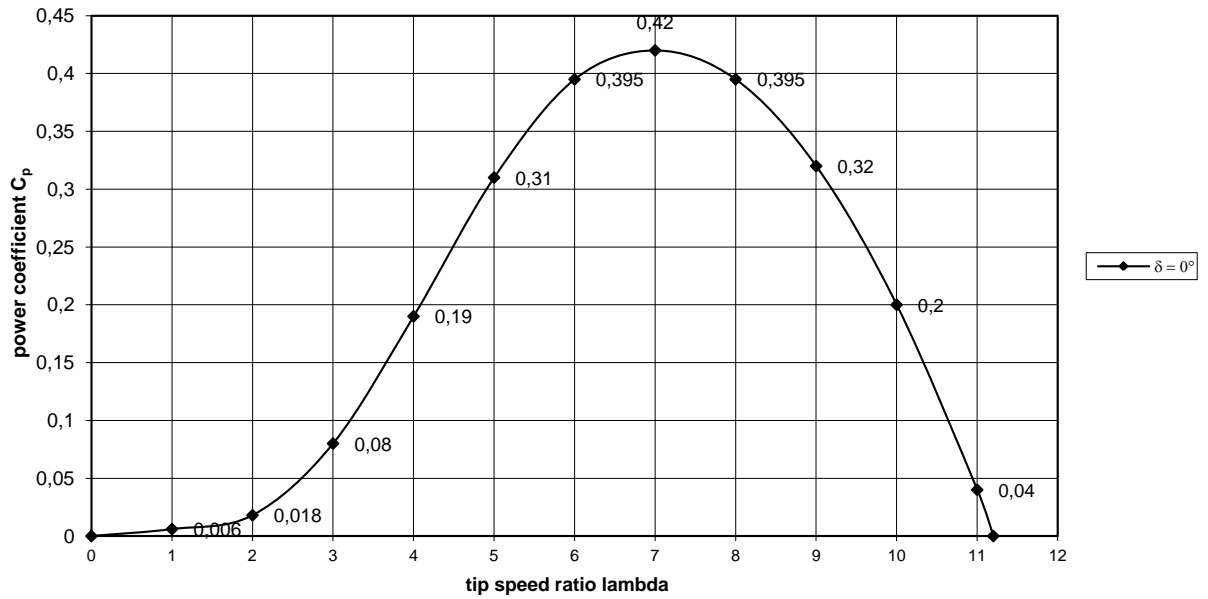


fig. 2 Estimated  $C_p$ - $\lambda$  curve for the VIRYA-5 rotor for the wind direction perpendicular to the rotor ( $\delta = 0^\circ$ )

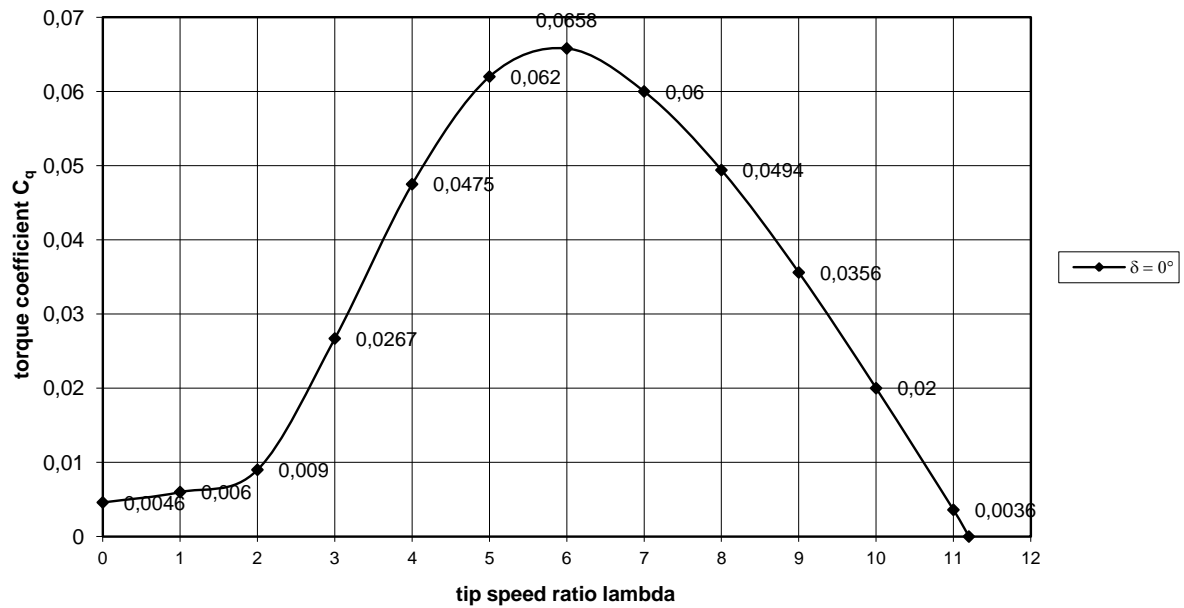


fig. 3 Estimated  $C_q$ - $\lambda$  curve for the VIRYA-5 rotor for the wind direction perpendicular to the rotor ( $\delta = 0^\circ$ )

## 5 Determination of the P-n curves, the optimum cubic line and the lines for constant f

The determination of the P-n curves of a windmill rotor is described in chapter 8 of KD 35. One needs a  $C_p$ - $\lambda$  curve of the rotor and the characteristics of the safety system together with the formulas for the power P and the rotational speed n. For the hinged side vane safety system, the  $\delta$ -V curve can be estimated. For a pitch control safety system, it is rather difficult to determine what effect, a certain increase of the blade angle  $\beta$  has on the rotor characteristics. Therefore at this moment it is assumed that the rotor characteristics are not changed up to a wind speed of 10 m/s. So the P-n curves of the rotor are drawn up to this wind speed for a rotor perpendicular to the wind. The safety system starts to be active above a certain rotational speed and the effect of this on the P-n curves of the rotor will be discussed in chapter 9. The  $C_p$ - $\lambda$  curve is given in figure 2.

The P-n curves are used to check the matching with the  $P_{mech}$ -n curve of the generator for a certain gear ratio i (the VIRYA-5 has no gearing so  $i = 1$ ). Because we are especially interested in the domain around the optimal cubic line and because the P-n curve for low values of  $\lambda$  appear to lie very close to each other, the P-n curves are not determined for low values of  $\lambda$ . The P-n curves are determined for wind the speeds 3, 4, 5, 6, 7, 8, 9 and 10 m/s.

Substitution of  $R = 2.5$  m in formula 4.8 of KD 35 gives:

$$n = 3.8197 * \lambda * V \quad (\text{rpm}) \quad (8)$$

Substitution of  $\rho = 1.2$  kg / m<sup>3</sup> and  $R = 2.5$  m in formula 4.1 of KD 35 gives:

$$P = 11.781 * C_p * V^3 \quad (\text{W}) \quad (9)$$

The P-n curves are determined for  $C_p$  values belonging to  $\lambda$  is 4, 5, 6, 7, 8, 9, 10 and 11.2 (see figure 1). For a certain wind speed, for instance  $V = 3$  m/s, related values of  $C_p$  and  $\lambda$  are substituted in formula 8 and 9 and this gives the P-n curve for that wind speed.

		V = 3 m/s		V = 4 m/s		V = 5 m/s		V = 6 m/s		V = 7 m/s		V = 8 m/s		V = 9 m/s		V = 10 m/s	
$\lambda$ (-)	$C_p$ (-)	n (rpm)	P (W)	n (rpm)	P (W)	n (rpm)	P (W)	n (rpm)	P (W)	n (rpm)	P (W)	n (rpm)	P (W)	n (rpm)	P (W)	n (rpm)	P (W)
4	0.19	45.8	60.9	61.1	143.3	76.4	279.8	91.7	483.5	107.0	767.8	122.2	1146	137.5	1632	152.8	2238
5	0.31	57.3	99.4	76.4	233.7	95.5	456.5	114.6	788.9	133.7	1253	152.8	1870	171.9	2662	191.0	3652
6	0.395	68.8	126.6	91.7	297.8	114.6	581.7	137.5	1005	160.4	1596	183.3	2383	206.3	3392	229.2	4655
7	0.42	80.2	134.6	107.0	316.7	133.7	618.5	160.4	1069	187.2	1697	213.9	2533	240.6	3607	267.4	4948
8	0.395	91.7	126.6	122.2	297.8	152.8	581.7	183.3	1005	213.9	1596	244.5	2383	275.0	3392	305.6	4655
9	0.32	103.1	102.6	137.5	241.3	171.9	471.2	206.3	814.3	240.6	1293	275.0	1930	309.4	2748	343.8	3770
10	0.2	114.6	64.1	152.8	150.8	191.0	294.5	229.2	508.9	267.4	808.2	305.6	1206	343.8	1718	382.0	2356
11.2	0	128.3	0	171.1	0	213.9	0	256.7	0	299.5	0	342.2	0	385.0	0	427.8	0

table 2 Calculated values of n and P as a function of  $\lambda$  and V for the VIRYA-5 rotor

The calculated values for n and P are plotted in figure 4. The optimum cubic line which can be drawn through the tops of the P-n curves, is also given in figure 4.

The 34-pole generator has not yet been built and measured, so measured characteristics are not available. However, it is possible to derive the lines for which the frequency has a certain value. A 2-pole PM-generator has a frequency of 50 Hz for a rotational speed of 3000 rpm. So a 34-pole generator has a frequency of 50 Hz for a rotational speed of  $3000 * 2 / 34 = 176.47$  rpm. As the frequency is proportional to the rotational speed, the rotational speeds for other frequencies can be determined easily. It is found that:



$n = 123.53$  rpm for  $f = 35$  Hz.  
 $n = 141.18$  rpm for  $f = 40$  Hz.  
 $n = 158.82$  rpm for  $f = 45$  Hz.  
 $n = 176.47$  rpm for  $f = 50$  Hz.  
 $n = 194.12$  rpm for  $f = 55$  Hz.  
 $n = 211.76$  rpm for  $f = 60$  Hz.  
 $n = 229.41$  rpm for  $f = 65$  Hz.

The lines for constant frequencies of 35, 40, 45, 50, 55, 60 and 65 Hz are also given in figure 4. In figure 4 it can be seen that the line for  $f = 50$  Hz is intersecting with the optimum cubic line at a power of about 1490 W. The available electrical power will be lower because of the generator efficiency. Assume the generator efficiency is 0.8, so the electrical power is about 1192 W. This power is generated at a wind speed of about 6.7 m/s. The wind speed for which the line for 50 Hz is intersecting with the optimum cubic line is called the design wind speed  $V_d$ . So  $V_d = 6.7$  m/s.

A centrifugal pump with a 1.1 kW pump motor used at a factor 0.8 of its nominal power and with a motor efficiency of 0.75 will absorb an electrical power of about 1170 W, so a 1.1 kW pump motor seems an acceptable choice. The working point will lie about on the optimum cubic line for a pump with a 1.1 kW motor.

In figure 4 it can be seen that the power at a wind speed of 10 m/s and at a frequency of 50 Hz is about 3300 W. The maximum power at a wind speed of 10 m/s is almost 5000 W if the optimum cubic line is followed. The frequency is about 75 Hz which is much too high. The frequency is about 60 Hz at a wind speed of 8 m/s if the optimum cubic line is followed. So the pitch control system must prevent that the rotational speed becomes too high, even at moderate wind speeds.

Below a frequency of about 35 Hz, belonging to a rotational speed of 123.53 rpm, the pump is no longer able to produce the static water height, so no water will be pumped. Probably it is necessary to disconnect the generator and the pump motor by a 3-phase switch below a frequency of about 35 Hz. This makes that the rotor will always start unloaded at low wind speeds. If the connection is broken at  $f = 35$  Hz for a running rotor, this results in acceleration of the rotor. The connection can be made at a frequency of 50 Hz belonging to a rotational speed of about 176 rpm. This frequency will be reached for an unloaded rotor for a wind speed of about 4.2 m/s. So the pump will start pumping at this wind speed but it will stop only if the frequency becomes lower than 35 Hz. This means that even at low wind speeds there will be some intermittent output.

If the pump is a centrifugal pump, the system will probably also work if there is no 3-phase switch which disconnects the generator and the pump motor but in this case water is not pumped intermittently if the wind speed is just above 4.2 m/s. A switch will certainly be needed for a positive displacement pump as such pump demands a torque directly from stand still position.

The generator winding must be chosen such that the loaded voltage is 230 V at a frequency of 50 Hz. This means that the unloaded voltage at 50 Hz must be a lot higher. I expect about 280 V but this must be tested for a prototype of the generator.

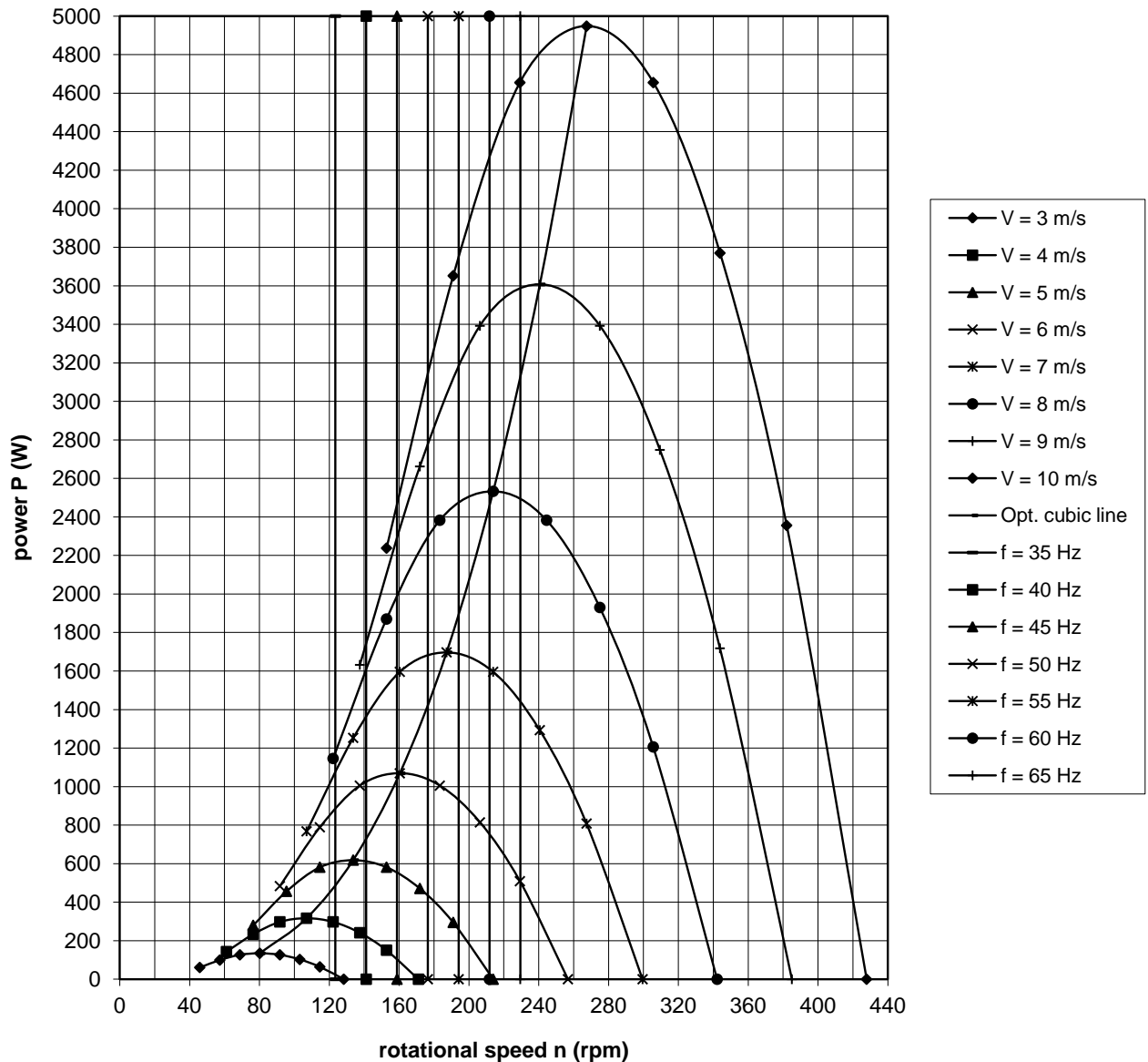


fig. 4 P-n curves of the VIRYA-5 rotor, optimum cubic line and line for frequencies  $f$  of 35, 40, 45, 50, 55, 60 and 65 Hz

## 6 Description of the 34-pole PM-generator (see figure 5)

The number of stator poles for a 3-phase winding must be dividable by 3. The armature must have an even number of poles. If there is only a difference of one in between the number of stator poles and the number of armature poles it means that the number of stator poles must be odd. So the number of stator poles can be 3, 9, 15, 21, 27, 33, 39, 45, 51, 57, 63, 69, 75 etc. None of these values matches with the available number of stator poles for standard stator stampings of asynchronous motors. This problem can be solved by doubling the required number of stator and armature poles. The difference in between the number of stator poles and the number of armature poles must now be two. Doubling of the number of armature poles means that the number of armature poles is always even, also if the number of stator poles is even. In this case the required number of stator poles can be 6, 12, 18, 24, 30, 36, 42, 48, 54, 60, 66, 72 etc. So the numbers 24, 36, 48, 54 and 72 match with available numbers for standard stator stampings.

If the number of armature poles is two more than the number of stator poles it is respectively 26, 38, 50, 56 and 74. If the number of armature poles is two less than the number of stator poles it is respectively 22, 34, 46, 52 and 70.

The number of armature poles must be chosen rather high for the VIRYA-5 to realise an acceptable low design wind speed. It is chosen to take 36 stator poles and 34 armature poles. The rotational speed for a 2-pole generator is 3000 rpm for a frequency of 50 Hz. So for a 34-pole generator, the frequency is 50 Hz for a rotational speed of  $3000 * 2 / 34 = 176.47$  rpm or for 2.94 revolutions per second. In figure 4 it can be seen that  $n = 176.47$  rpm results in a design wind speed of about 6.7 m/s which is a reasonable choice for a moderate wind regime.

The coil configuration of the VIRYA-5 generator is chosen the same as for the VIRYA-3.3S generator. So the coil configuration over  $360^\circ$  will be: 3 coils U, 3 coils W, 3 coils V, 3 coils U, 3 coils W and 3 coils V. A coil is wound around one stator spoke so every coil makes use of two adjacent stator grooves. All 18 coils are identical and are lying in one cylinder shaped plane, so there are no crossing coil heads

The stator pole angle for 36 stator poles is  $360^\circ / 36 = 10^\circ$ . The angle in between the coils is the double value so  $360 / 18 = 20^\circ$ . The armature pole angle for 34 armature poles is  $360^\circ / 34 = 10.5882^\circ$ .

The angle between two north poles is the double value so  $360 / 17 = 21.1765^\circ$ . The difference in between the stator pole angle and the armature pole angle is  $10.5882^\circ - 10^\circ = 0.5882^\circ$ . Assume a preference position is created if an armature pole is just opposite a stator pole. This means that the number of preference positions per revolution is  $360^\circ / 0.5882 = 612$ . This is a very large number so it can be expected that the fluctuation of the clogging torque can be neglected. The number of preference positions can also be found by multiplying the number of armature poles and stator poles and divide it by two as  $34 * 36 / 2 = 612$ .

Provisionally it is chosen to make use of a motor housing which makes use of a stator stamping of manufacture Kienle and Spiess. The manufacturer which uses stampings of Kienle and Spiess for their motors has not yet been chosen. Information about the geometry of these stampings is given on the website: [www.kienle-spiess.de](http://www.kienle-spiess.de). The largest stator stamping with 36 stator grooves is used for a 6-pole motor frame size 132 M. The longest stator stamping is used for a 5.5 kW motor. This stator stamping has an inside diameter of 135 mm, an outside diameter of 200 mm and a length of 180 mm. The armature stamping has an inside diameter of 50 mm but the armature stamping is not used.

The armature diameter is chosen 134.2 mm, so the air gap in between armature and stator is 0.4 mm. The armature length is chosen the same as the stator length, so 180 mm.

Some research has been done to neodymium magnets which are standard supplied by Internet companies and which can be used for this new generator type. The company [www.enesmagnets.pl](http://www.enesmagnets.pl) supplies magnets size  $30 * 10 * 8$  mm with quality N40H. The current price (including VAT, excluding transport) is € 1.43 per magnet for 140 magnets.

The armature is made from a mild steel cylinder with a diameter of 134.2 mm and a length of 180 mm. In this cylinder 17, 10 mm wide and 8.3 mm deep grooves are made parallel to the axis. Six magnets are glued in each groove, so 102 magnets are needed for one armature. The magnet costs are about € 150 which seems acceptable. All magnets are glued with the north pole to the outside.

The south poles are formed by the remaining material in between the grooves. A 2.4 mm wide and 5.3 mm deep groove is made at each side of a magnet. This groove makes that a south pole also has a width of about 10 mm and that there is no magnetic short-circuit in between the sides of the magnets. The 17 north poles are called N1 - N17. The 17 south poles are called S1 – S17. A picture of armature and stator is given in figure 5. The position of the armature in figure 5 is drawn such that north pole N1 is just opposite coil U2.

The shaft can be made using the original motor shaft. So the shaft will also get a fine teething. The armature is pressed over the teething. The sheets of the original armature stamping have a central hole with a diameter of 50 mm. As the lamination is rather soft, a little larger inside diameter has to be used for the mild steel bush of the armature, other wise the required pressing force will be too high. It is expected that this must be 50.2 mm.

For small series, the armature must be made from massive bar. However, for big series it might be possible to make the armature also from sheet lamination which is already provided with the pattern of the grooves for the magnets.

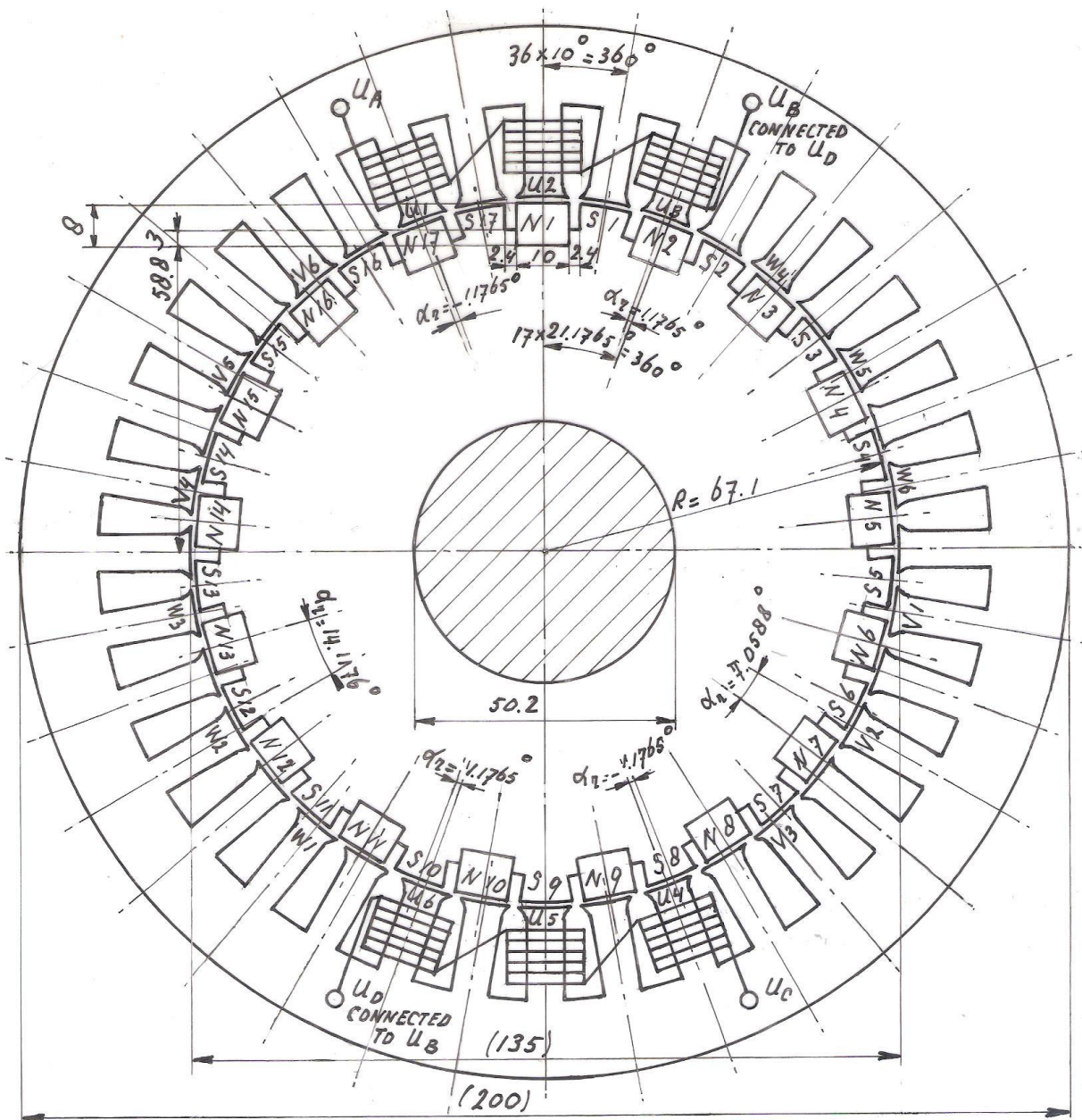


figure 5 34-pole armature and 36-pole stator for housing size 132M, 200 \* 135 \* 50 mm

## 7 Checking if a 3-phase current is generated

A 3-phase current has three phases called U, V and W. Normally the voltage U of each phase varies sinusoidal and the angle  $\alpha$  in between the phases is  $120^\circ$ . The formulas for the voltage of each phase are:

$$U_u = U_{\max} * \sin\alpha \quad (\text{V}) \quad (10)$$

$$U_v = U_{\max} * \sin(\alpha - 120^\circ) \quad (\text{V}) \quad (11)$$

$$U_w = U_{\max} * \sin(\alpha - 240^\circ) \quad (\text{V}) \quad (12)$$

The three curves are shown in figure 6.

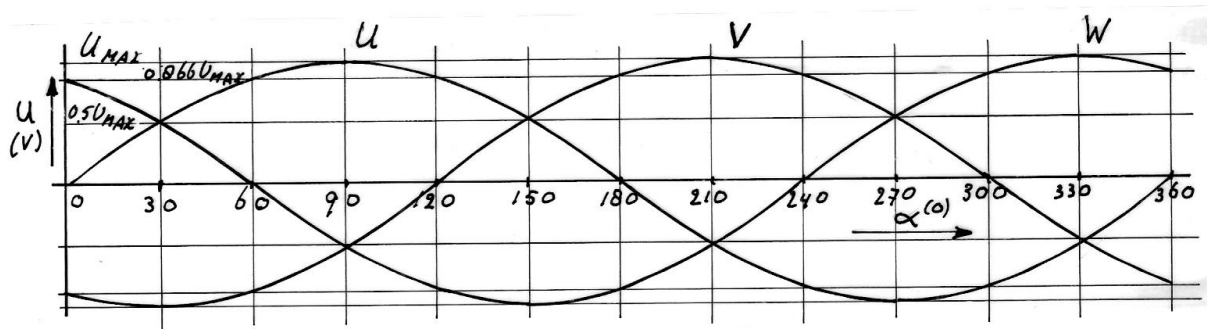


fig. 6 Three phases U, V and W

A pure sine wave is generated if a coil is rotating in a constant magnetic field because the magnetic field through the coil varies sinusoidal. If a permanent magnet is moving along a coil, the generated voltage may not be a pure sine wave, especially if the distance in between the magnets is large. But for the chosen generator configuration it is assumed that the generated voltage varies about sinusoidal.

If the rotor has two poles, the position of the rotor with respect to the stator will be the same if the rotor has rotated  $360^\circ$ . So the phase angle  $\alpha$  is the same as the rotational angle  $\alpha_r$  of the rotor. If the rotor has 34 poles this will be the case for  $360 * 2 / 34 = 21.1765^\circ$  rotation of the rotor. This results in the formula:

$$\alpha = \alpha_r * p_r / 2 \quad (-) \quad (13)$$

$\alpha$  is the phase angle,  $\alpha_r$  is rotational angle of the rotor and  $p_r$  is the number of rotor poles.

In figure 5 it can be seen that  $\alpha_r = 0^\circ$  in between N1 and U2, that  $\alpha_r = 7.0588^\circ$  in between N7 and V2 and that  $\alpha_r = 14.1176^\circ$  in between N13 and W2. Substitution of  $\alpha_r = 0^\circ$  and  $p_r = 34$  in formula 13 gives  $\alpha = 0^\circ$ . Substitution of  $\alpha_r = 7.0588^\circ$  and  $p_r = 34$  in formula 13 gives  $\alpha = 120^\circ$ . Substitution of  $\alpha_r = 14.1176^\circ$  and  $p_r = 34$  in formula 13 gives  $\alpha = 240^\circ$ . The difference in between the phase angles is  $120^\circ$  and so a 3-phase voltage is created in between the coils U2, V2 and W2.

In figure 5 it can be seen that  $\alpha_r = -1.1765^\circ$  in between N17 and U1 and that  $\alpha_r = 1.1765^\circ$  in between N2 and U3. So this means that the voltages generated in U1 and U3 are not in phase with the voltage generated in U2.

In figure 5 it can be seen that the coils U4, U5 and U6 are not about opposite to north poles but that they are about opposite to the south poles S8, S9 and S10. This means that the generated voltage in this bundle of coils will be opposite to the voltage as generated in the bundle of coils U1, U2 and U3 if the coils have the same winding direction. It is decided to give all 18 coils the same winding direction and to connect all six coils of one phase in series. The coil ends of the bundle of the three coils U1, U2 and U3 are called  $U_A$  and  $U_B$ . The coil ends of the bundle of the three coils U4, U5 and U6 are called  $U_C$  and  $U_D$ . The first bundle of 3 coils of phase U has to be connected such to the second bundle of 3 coils, that the generated voltages in both bundles are strengthening each other. This is realised if coil end  $U_B$  is connected to  $U_D$ .

The generator winding is very simple if compared to the winding of a normal 6-pole asynchronous motor. This is because all coils have the same shape and because there are no crossing coil heads. The strength of the magnetic field flowing through a coil will be the same for each coil and the generated voltage in each coil will therefore be the same too. This is not the case for a normal 6-pole winding as some coils have a different pitch. The coil heads are very small if compared to the length of the part of the coil lying in the grooves. A minimum amount of copper will therefore be used and the winding will have a relatively low resistance resulting in a high generator efficiency.

The angles in between the coils U4 – U6 and the poles S8 – S10 are the same as the angles in between the coils U1 – U3 and the poles N17 – N2.

Coil U1 and U4. Substitution of  $\alpha_r = -1.1765^\circ$  and  $p_r = 34$  in formula 13 gives  $\alpha = -20^\circ$ .

Coil U3 and U6. Substitution of  $\alpha_r = 1.1765^\circ$  and  $p_r = 34$  in formula 13 gives  $\alpha = 20^\circ$ .

Addition of sinusoidal voltages which are out of phase but which have the same frequency results in a voltage which is also sinusoidal. The total voltage  $U_{tot}$  for the six coils U1 – U6 is given by:

$$U_{tot} = U_{max} * 2 * \{ \sin(\alpha - 20^\circ) + \sin \alpha + \sin(\alpha + 20^\circ) \} \quad (V) \quad (14)$$

It can be proven that this function has a maximum value for  $\alpha = 90^\circ$ . Substitution of  $\alpha = 90^\circ$  in formula 14 gives:

$$U_{tot \max} = U_{max} * 2 * (\sin 70^\circ + \sin 90^\circ + \sin 110^\circ) = 5.7588 * U_{max}.$$

If the voltages U1 - U6 would be exactly in phase, the resulting maximum voltage would be  $6 * U_{max}$ . So the difference in phase angle gives a small reduction of the total voltage by a factor  $5.7588 / 6 = 0.960$  and therefore also a small reduction of the generated power. A factor 0.960 is certainly acceptable, so the given shift of the phase angles in between the three coils of a bundle U is allowed. The same counts for the coils V and W.

Probably a 3-phase relay in between the generator and the pump motor is needed to realise that the windmill starts unloaded. The relay is activated by the generator frequency.

In stead of use in combination with a pump motor it is possible to use the generator for high voltage battery charging. If the voltage for the standard winding is too high, the voltage is halved if the bundle of three coils of one phase is connected in parallel to the other bundle of three coils of the same phase. In this case coil end  $U_A$  has to be connected to coil end  $U_D$  and coil end  $U_B$  has to be connected to coil end  $U_C$ . For 24 V battery charging, one will need a special winding with a much lower number of turns per coil and a much larger wire thickness.

Rectification in star will give the lowest sticking torque because higher harmonic currents can't circulate in the winding. If the generator is used as a brake, the star point should be short-circuited too because this gives a higher maximum braking torque. Because the frequency is high, it might be required to make short-circuit over a resistor to create a torque which is high enough at normal rotational speeds.

## 8 Calculation of the flux density in the air gap and the stator spokes

A PM-generator is normally designed such that the magnetic field in the stator is saturated or almost saturated. For this condition, the generator has its maximum torque level and this means that it can supply the maximum electrical power for a certain rotational speed. The stator can be saturated at the narrowest cross section of the spokes in between the stator slots but it can also be saturated at the bridge in between the bottom of the stator slots and the outside of the stator stamping. The stator stamping is originally designed for a 6-pole motor and for a 6-pole motor there is a large magnetic flux in the bridge. The magnetic flux in the bridge for a 34-pole PM-generator is very low because only half the flux coming out of one a stator pole is flowing through the bridge. So only the magnetic flux in the spokes is critical. The stator is about saturated if the calculated flux density in the air gap is 0.9 T or higher.

The remanence  $B_r$  (magnetic flux) in a neodymium magnet supplied by Enesmagnets with quality N40H is in between 1.26 T and 1.29 T, if the magnet is short-circuited with a mild steel arc which is not saturated. Assume it is 1.275 T. However, an air gap in the arc reduces the magnetic flux because it has a certain magnetic resistance. The resistance to a magnetic flux for the magnet itself is about the same as for air. The magnet thickness is called  $t_1$ . The magnetic resistance of the iron of the armature can probably be neglected. The magnetic resistance of the iron in the stator can't be neglected if the stator is close to saturation. However, this is complicating the calculation a lot and so the magnetic resistance of the iron in the stator is also neglected. So the total magnetic resistance is only caused by the magnet itself and by the air gaps.

The air gap  $t_2$  in between a south pole and the stator is 0.4 mm. The average air gap  $t_3$  in between a north pole and the stator is somewhat larger because the magnet is flat and because the depth of a magnet groove is chosen 8.3 mm. It is assumed that  $t_3 = 0.6$  mm. So the magnetic resistance is increased by a factor  $(t_1 + t_2 + t_3) / t_1$  because of the two air gaps. This means that the remanence in the air gap is reduced by a factor  $t_1 / (t_1 + t_2 + t_3)$ . The effective remanence in the air gap  $B_{r\text{eff}}$  is given by:

$$B_{r\text{eff}} = B_r * t_1 / (t_1 + t_2 + t_3) \quad (\text{T}) \quad (15)$$

Substitution of  $B_r = 1.275$  T,  $t_1 = 8$  mm,  $t_2 = 0.4$  mm and  $t_3 = 0.6$  mm in formula 15 results in  $B_{r\text{eff}} = 1.133$ . This is higher than 0.9 T so the stator will probably be saturated. The flux density in a spoke can be calculated if the spoke width is known. The spoke width is about 7 mm. As a magnet has a width of 10 mm, the magnetic flux is concentrated by a concentration factor  $k = 10 / 7 = 1.429$ . So the magnetic flux in a spoke can be calculated to be  $1.429 * 1.133 = 1.62$  T. This is higher than 1.6 T so the spokes are saturated and the maximum possible torque level will be realised.

I think that it is worth while to make a prototype of a stator and an armature according to the geometry as given in figure 5 and chapter 6 and to test if the generator will have acceptable characteristics. The optimum number of windings per coil and the wire thickness are found by try and error. The open phase voltage must be a lot higher than 230 V for a frequency of 50 Hz as the loaded phase voltage must be about 230 V. A frequency of 50 Hz is realised for a rotational speed of 176.47 rpm.

First a half winding with three coils of one phase is laid with a thin wire with for instance 100 windings per coil. Assume one measures an open AC voltage of 100 V for  $f = 50$  Hz. So the voltage for a whole winding with six coils would be 200 V. Assume an open voltage of 280 V at 50 Hz is needed. So the number of windings has to be increased by a factor  $280 / 200 = 1.4$  and becomes 140 windings per coil. Next one selects the maximum wire thickness for which 140 windings can be laid in a groove and one manufactures a complete 3-phase winding with this wire thickness. Next the generator is measured in combination with a loaded pump motor and it is investigated if the loaded phase voltage is about 230 V at 50 Hz.

It might be possible to use this idea of a 34-pole PM-generator for a 34-pole synchronous PM-motor with a high torque level at a low rotational speed. Such motor can be used for direct drive of an electrical car. One needs a power source which supplies a 3-phase current with variable frequency. The rotational speed will be 176.47 rpm for  $f = 50$  Hz.

## 9 Description of the pitch control mechanism

### 9.1 general aspects of pitch controls systems

The blade angle  $\beta$  is sometimes called the pitch angle. So a pitch control system is a safety system which uses variation of the blade angle to limit the maximum rotational speed and the maximum power. The limitation can be realised by two directions of blade rotation. Rotation of the blade to smaller blade angles is called negative pitch control or active stall. Rotation of the blade to larger blade angles is called positive pitch control.

Rotation of the blade to smaller blade angles results in increase of the angle of attack  $\alpha$ . At a certain value of  $\alpha$ , the maximum lift coefficient  $C_{l\max}$  is reached and this is the angle  $\alpha_{st}$  where stalling starts. For higher angles  $\alpha$ , and so for smaller angles  $\beta$ ,  $C_l$  decreases somewhat but the drag coefficient  $C_d$  increases strongly if  $\alpha$  is higher than  $\alpha_{st}$ . At a certain angle  $\beta$ , the component of the drag opposed to the direction of rotation will become larger than the component of the lift in the direction of rotation (see KD 35 figure 4.4 and formula 4.14). This means that all generated power will be used to overcome the airfoil drag. So no mechanical power can be generated on the rotor shaft and this means that the rotor will slow down if the generator withdraws power from the rotor.

The VIRYA-5 rotor is designed with a high lift coefficient at the blade root and a low lift coefficient at the blade tip. So the stalling point will move from the inside of the blade to the outside of the blade if the blade angle is decreased.

#### Advantages of negative pitch control

- 1) Only a rather small maximum decrease of the blade angle (about  $10^\circ$ , so  $\beta = -4^\circ$ ) is needed to realise stall for the almost the whole blade length.
- 2) A sudden wind gust results in a sudden increase of the angle of attack  $\alpha$ . So only a little variation in the blade angle is required to realise stalling for a large part of the blade length.
- 3) If variation of the blade angle is also used to increase the starting torque, one can go from a large blade angle at starting to a small blade angle at the normal design tip speed ratio and then to a negative blade angle at stalling, using one mechanism working in the same direction.

#### Disadvantages of negative pitch control

- 1) It results in increase of the rotor thrust especially at the blade tip.
- 2) A stalling blade may be rather noisy.
- 3) The aerodynamic moment is working in a direction which has a tendency to increase the blade angle. So a rather large pitch moment is needed to overpower the aerodynamic moment. If this pitch moment is supplied by centrifugal weights, rather large weights will be needed.

Rotation of the blade to larger blade angles results in decrease of the angle of attack  $\alpha$ . A smaller angle  $\alpha$  result in decrease of the lift coefficient and so in decrease of the generated torque. So if the generator loads the rotor with a certain torque, the rotational speed will decrease.



### **Advantages of positive pitch control**

- 1) The aerodynamic moment works in a direction which has a tendency to increase the blade angle. So the aerodynamic moment can be used to activate the pitch control system. If the aerodynamic moment is not large enough, relative small centrifugal weights are needed to give some extra pitch moment.
- 2) This system results in decrease of the lift coefficient so in decrease of the rotor thrust and so in decrease of the forces on the tower and the foundation.
- 3) The rotor stops rotating for  $\beta = 99^\circ$  ( $C_1 = 0$ ,  $\alpha = -9^\circ$ ). So no brake is needed for  $\beta = 99^\circ$ .

### **Disadvantages of positive pitch control**

- 1) A rather large increase of the blade angle of about  $20^\circ$  is needed (so  $\beta = 26^\circ$ ) to limit the rotational speed enough at very high wind speeds.
- 2) A sudden wind gust results in a sudden increase of the angle of attack  $\alpha$ . So a large blade angle will be needed to realise a blade angle  $\alpha$  which is small enough to compensate the wind gust.
- 3) The blade can move to a larger angle  $\beta$  if the rotor is stopped (see chapter 9.8). This is because the drag at a large angle  $\alpha$  exerts about at half the chord from the airfoil nose.

Apart from aerodynamic forces and centrifugal forces also the force due to the weight of the centrifugal weights, is active. The direction of this force with respect to the position of the blade varies  $360^\circ$  during one blade rotation. This will cause some variation of the blade angle. To prevent this variation, it is necessary that the movements of all blades are synchronised by the pitch control mechanism if a centrifugal weight is used for the pitch control system. However, if the pitch control system is only activated by the aerodynamic moment, the situation is different.

The aerodynamic moment for a certain blade section is determined by the relative wind speed  $W$ . The relative wind speed  $W$  is illustrated in figure 5.1 of KD 35 and is the vector sum of the local blade speed  $\Omega * r$  and the absolute wind speed in the rotor plane  $2/3 V$  (if the wake rotation is neglected). For rotors with a high design tip speed ratio like the VIRYA-5 rotor,  $\Omega * r$  is large with respect to  $2/3 V$  which means that  $W$  is only a little larger than  $\Omega * r$ . So even if the absolute wind speed isn't constant for the whole rotor plane,  $\Omega * r$  will be almost constant for a certain value of  $r$  and this means that  $W$  will be almost constant for a certain rotational speed. This means that the increase of the blade angle will be the same for both blades if the friction of the pitch control system is the same for each blade and so no synchronisation mechanism is required.

Pitch variation can be steered by the aerodynamic moment, by a pitch moment which is caused by centrifugal weights or by an external energy source. Modern very large 3-bladed windmills generally use an external source and a computer for each windmill. The pitch variation of all three blades is synchronised by a system of levers on each of the blade roots. The rotor shaft is hollow and contains a pin which is connected to the blade levers. The blades can rotate more than  $90^\circ$  if the pin is moved front- or backwards. The movement of the pin is caused by a hydraulic cylinder which is steered by the rotational speed or by the generated power. But any signal can be used to activate the pitch control system. The system can be used to stop the rotor for a positive blade angle of about  $99^\circ$ . It can also be used to facilitate starting, by slowly decreasing the blade angle if the rotor is accelerating.

An important disadvantage of this system is that it only works as long as energy is available to power the hydraulic system. If this energy is directly taken from the grid, the whole system will fail if the grid falls off. So some back up power is needed. Another disadvantage is that the system only works if the computer and if the hydraulics works. If there is a break down in one of these systems, the pitch control system will fail and the rotor may rotate that fast that it can be destroyed. This system is certainly too complicated and too expensive for the VIRYA-5 windmill.

## 9.2 Choices made for the pitch control system of the VIRYA-5

It is expected that certain developing countries will be interested to build the VIRYA-5. But as the possibilities of manufacture in these countries will be limited, the pitch control system must be as simple and as cheap as possible. The next choices were made.

- 1 A rotor with only two blades is used. A rotor with two blades allows that both blade shafts are in parallel to each other and that the blade bearings can be connected to one central connecting strip. Therefore the whole pitch control mechanism will be rather compact.
- 2 Positive pitch control, activated by only the aerodynamic moment, will be used. So no centrifugal weights will be used like it is often done for pitch control systems of small wind turbines. The axis of the blade shaft will be chosen as close as possible to the quarter chord point of the airfoil.
- 3 The blade shaft will be made of 30 mm square stainless steel bar with 20 mm shaft ends at both sides. A blade shaft is bolted to the blade by two M16 bolts. Two bearing housings for each blade, also made out of 30 mm square stainless steel bar, are mounted to the back side of the connecting strip. An INA Permaglide bronze plain bearing with an inner diameter of 20 mm and a length of 20 mm is pressed in each bearing housing and each end of the blade shaft rotates in such bearing.
- 4 The centrifugal force in the blade is rather high for the rotational speed for which the blade starts pitching, so use of a flanged INA Permaglide bearing to take the centrifugal force is not allowed as it will give too much friction. So a stainless steel thrust ball bearing size  $\phi 20 * \phi 35 * 10$  mm is used to take the centrifugal force.
- 5 There is no synchronisation mechanism which makes that the variation of the blade angle is exactly the same for both blades. If the spring is adjusted to the same force for both blades, it can be expected that the variation of the blade angle will also be the same for both blades. This makes the whole system a lot simpler than the mechanism which was designed for the VIRYA-15 rotor.
- 6 The pitch movement starts at a loaded rotational speed of 187 rpm. This rotational speed corresponds to a frequency of about 53 Hz. This rotational speed is realised for a wind speed of 7 m/s if the optimum cubic line is followed (see figure 5). It is expected that the system is that sensible that the maximum frequency will become not higher than about 58 Hz. To realise this, only a little friction in the bearings is allowed and the spring which pushes the blade to the neutral position must be rather weak.
- 7 The blade can rotate over  $20^\circ$ , so the maximum blade angle will be  $26^\circ$ . It is expected that  $\beta = 26^\circ$  results in a reduction of the tip speed ratio which is enough to effectively limit the rotational speed of the rotor, even for very high wind speeds.
- 8 The outer 2000 mm of a blade will be provided with the Gö 711 airfoil. The inner 350 mm will only be equipped with two bevelled edges which touch the airfoil geometry. So this means that these two bevelled edges can be made by a plane shaving machine for the whole blade and that the real airfoil is made in the outer 2000 mm afterwards.
- 9 For the inner 350 mm, a flat part remains in between the two bevelled edges which is in parallel to the flat front side of the blade. This flat part is used for the connection of the bolts of the blade shaft. A 3 mm thick and 30 mm wide stainless steel strip is used at both sides of the blade. On the back side, this strip prevents that the bolt heads damage the wood. On the front side, the strip prevents that the thrust ball bearing touches the wood of the blade.
- 10 A lever is connected to the middle of the blade shaft and a compression spring pushes the blade to the neutral position. A supporting beam is mounted to the small side of the connecting strip to support the spring. A sketch of the connection of blade and shaft and of the bearing housing to the central strip is given in figure 7.

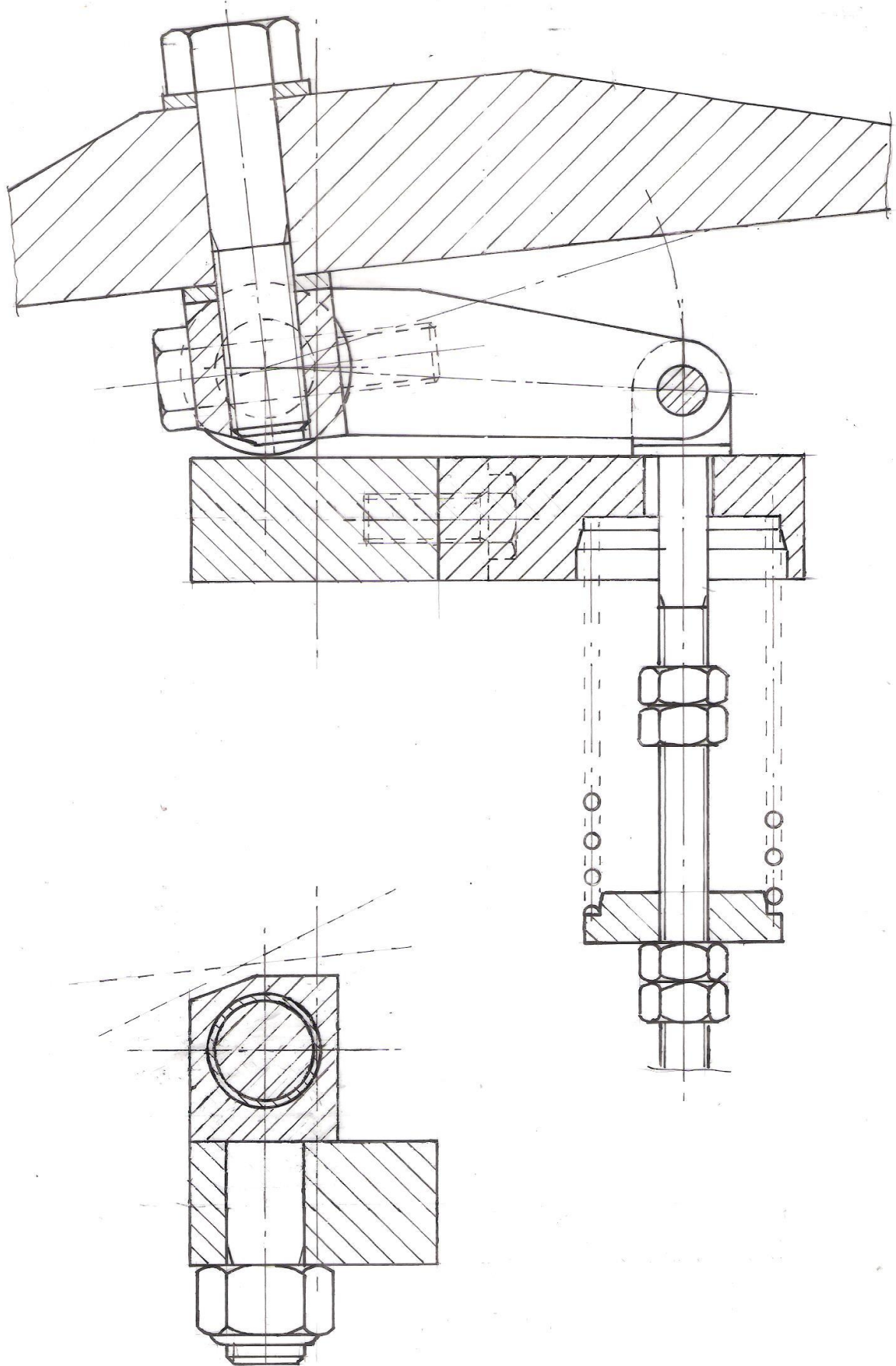


fig. 7 Connection of the blade shaft to the blade and of the bearing houses to the connecting strip

### 9.3 Determination of the aerodynamic moment and the spring force

The aerodynamic moment  $M$  depends on the aerodynamic moment coefficient  $C_m$ , the blade dimensions and the relative wind speed  $W$  which is felt by the blade. The  $C_{m0.25}-\alpha$  curve of the Gö 711 airfoil is given in figure 6 of report KD 285 (ref. 5). The moment coefficient is given around the quart chord point and is therefore indicated as  $C_{m0.25}$ . In figure 6 of KD 285 it can be seen that  $C_{m0.25}$  is almost constant for  $-4^\circ < \alpha < 12^\circ$ . This is favourable because it simplifies the calculation of  $M$  and the system will be rather stable. However, because of the chosen blade connection, it is not possible that the blade axis coincides with the quart chord point. Formula 1 of KD 285 gives the formula to calculate  $C_{mh}$  around a certain point H. This formula is copied as formula 16.

$$C_{mh} = C_{m0.25} + p/c \{C_l \cos(\alpha + \gamma) + C_d \sin(\alpha + \gamma)\} \quad (-) \quad (16)$$

The blade axis is chosen as close as possible to the quart chord point which results in  $\gamma = 90^\circ$ . For the distance  $p$  we find that  $p = 18 \text{ mm}$  for the chosen blade connection. The blade chord  $c = 0.24 \text{ m} = 240 \text{ mm}$ . Substitution of these values in formula 16 gives:

$$C_{mh} = C_{m0.25} + 0.075 \{C_l \cos(\alpha + 90^\circ) + C_d \sin(\alpha + 90^\circ)\} \quad (-) \quad (17)$$

The  $C_l$ ,  $C_d$  and  $C_{m0.25}$  coefficients as a function of  $\alpha$  are given in table 2 of KD 285. This table is copied as table 3.

$\alpha$ (°)	$C_l$ (-)	$C_d$ (-)	$C_{m0.25}$ (-)	$\alpha + 90^\circ$ (°)	$C_l \cos(\alpha + 90^\circ)$	$C_d \sin(\alpha + 90^\circ)$	$C_{mh}$ (-)
-14.1	-0.173	0.1640	-0.0174	75.9	-0.0421	0.1591	-0.0086
-11.6	-0.083	0.1275	-0.0350	78.4	-0.0167	0.1249	-0.0269
-9.0	0.009	0.0928	-0.0554	81.0	0.0014	0.0917	-0.0484
-6.2	0.070	0.0587	-0.0912	83.8	0.0076	0.0584	-0.0863
-4.2	0.284	0.0299	-0.1236	85.8	0.0208	0.0298	-0.1198
-2.2	0.483	0.0165	-0.1174	87.8	0.0185	0.0165	-0.1148
0.0	0.665	0.0142	-0.1145	90.0	0	0.0142	-0.1134
2.1	0.843	0.0134	-0.1089	92.1	-0.0309	0.0134	-0.1102
4.3	1.019	0.0153	-0.1070	94.3	-0.0764	0.0153	-0.1116
6.6	1.190	0.0235	-0.1060	96.6	-0.1368	0.0233	-0.1145
8.8	1.361	0.0297	-0.1061	98.8	-0.2082	0.0294	-0.1195
11.3	1.479	0.0476	-0.1110	101.3	-0.2898	0.0467	-0.1292
14.3	1.478	0.1078	-0.1270	104.3	-0.3651	0.1045	-0.1465
17.8	1.354	0.2090	-0.1460	107.8	-0.4139	0.1990	-0.1621

table 3  $C_l$ ,  $C_d$ ,  $C_m$  and  $C_{mh}$  as a function of  $\alpha$  for  $Re = 4 * 10^5$

A column for  $\alpha + 90^\circ$ , for  $C_l \cos(\alpha + 90^\circ)$ , for  $C_d \sin(\alpha + 90^\circ)$  and for  $C_{mh}$ , which can be found using formula 17, is added to table 3.

Figure 6 of report KD 285 is now copied as figure 7. The calculated  $C_{mh}-\alpha$  curve is added to figure 7. It can be seen that both curves differ only slightly. In figure 7 it can be seen that  $C_{mh}$  is about -0.115 for  $-4^\circ < \alpha < 10^\circ$ . The moment coefficient is defined positive if it is clockwise. So a negative moment coefficient means that the really generated aerodynamic moment has an anti clockwise direction.

This means that  $C_{mh}$  has a tendency to decrease the angle of attack  $\alpha$  and so to increase the blade angle  $\beta$ . Therefore it supports a positive pitch control system.

If the columns for  $C_l \cos(\alpha + 90^\circ)$  and  $C_d \sin(\alpha + 90^\circ)$  are observed, it can be seen that  $C_d \sin(\alpha + 90^\circ)$  is always positive but it has a minimum for  $\alpha = 2.1^\circ$ .  $C_l \cos(\alpha + 90^\circ)$  is negative for very negative angles of  $\alpha$ , it is positive for  $-9^\circ < \alpha < 0^\circ$  and negative again for  $0^\circ < \alpha$ . The final contribution of  $C_l$  and  $C_d$  to  $C_{mh}$  is such that the  $C_{mh}-\alpha$  curve is lying higher than the  $C_{m0.25}-\alpha$  curve for about  $\alpha < 0^\circ$  and that the  $C_{mh}-\alpha$  curve is lying lower than the  $C_{m0.25}-\alpha$  curve for about  $\alpha > 0^\circ$ .

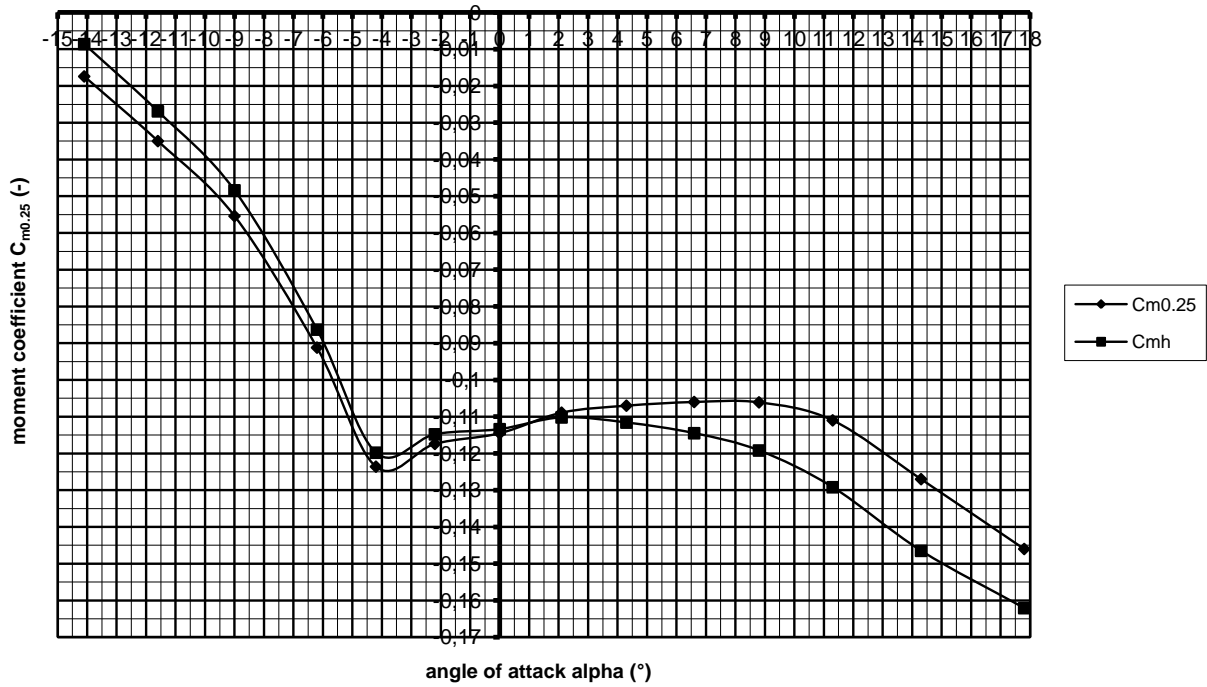


fig. 7  $C_{m0.25}-\alpha$  and  $C_{mh}-\alpha$  curve for Gö 711 airfoil for  $Re = 4 * 10^5$

The aerodynamic moment around point H,  $M_h$  is given by:

$$M_h = C_{mh} * \frac{1}{2} \rho W^2 * c^2 * b \quad (\text{Nm}) \quad (18)$$

In this formula,  $b$  is the airfoil width. Formula 18 is only valid if the airfoil is streamed by a wind speed  $W$  which is the same for the whole airfoil width. This is not the case for a rotating windmill blade. In this case the relative wind speed  $W$ , which is felt by the blade, differs for each station. If the wake rotation is neglected,  $W$  is given by formula 5.12 of KD 35. This formula is copied as formula 19.

$$W = V \sqrt{(\lambda_{rd}^2 + 4/9)} \quad (\text{m/s}) \quad (19)$$

Next the blade is divided into five sections 1 to 5 starting at the blade tip and each having a width  $b = 0.4$  m. The relative wind speed is calculated for the middle of a section, so at cross sections B, D, F, H and J and it is assumed that this wind speed can be used for the whole section. The values of  $\lambda_{rd}$  for a certain value of  $r$  can be derived from table 1. It is assumed that the rotor is loaded such by the generator that it runs at the design tip speed ratio  $\lambda_d = 7$ . So the hart of section 1 corresponds to station B with  $r = 2.3$  m and  $\lambda_{rd} = 6.44$ . The five sections and corresponding values of  $r$  and  $\lambda_{rd}$  are given in table 4.

Section	r (m)	$\lambda_{rd}$ (-)	W (m/s) for V = 7 m/s	$M_{hs}$ (Nm)
1	2.3	6.44	45.32	-3.265
2	1.9	5.32	37.53	-2.215
3	1.5	4.2	29.77	-1.409
4	1.1	3.08	22.06	-0.774
5	0.7	1.96	14.49	-0.334

table 4 r,  $\lambda_{rd}$ , W and  $M_{hs}$  as a function of the section number

W is calculated for a wind speed V = 7 m/s. Substitution of V = 7 m/s in formula 19 gives:

$$W = 7 \sqrt{(\lambda_{rd}^2 + 4/9)} \quad (\text{m/s}) \quad (\text{for } V = 7 \text{ m/s}) \quad (20)$$

The calculated values of W are also given in table 4. The angle of attack  $\alpha_{lin}$  varies in between  $-0.1^\circ$  for section 1 with r = 2.3 m and  $12^\circ$  for section 5 with r = 0.7 m (see table 1). It is assumed that a constant value  $C_{mh} = -0.115$  can be used for all five sections. Substitution of  $M_h = M_{hs}$  ( $M_{hs}$  is the contribution of a section),  $C_{mh} = -0.115$ ,  $\rho = 1.2 \text{ kg/m}^3$ , c = 0.24 m and b = 0.4 m in formula 18 gives:

$$M_{hs} = -0.00159 * W^2 \quad (\text{Nm}) \quad (\text{for } V = 7 \text{ m/s}) \quad (21)$$

Next  $M_{hs}$  is calculated for the values of W given in table 4 using formula 21. The calculated values of  $M_{hs}$  are also given in table 4. The total moment  $M_{hs \text{ tot}}$  is the sum of all calculated values of  $M_{hs}$ .

$$\text{So } M_{hs \text{ tot}} = \Sigma M_{hs} \quad (\text{Nm}) \quad (\text{for } V = 7 \text{ m/s}) \quad (22)$$

$$\text{So } M_{hs \text{ tot}} = -3.265 -2.215 -1.409 -0.774 -0.334 = -7.997 \text{ Nm}$$

The calculated value of  $M_{hs}$  for section 1 will be too high because of tip losses, so it is assumed that  $M_{hs \text{ tot}} = -7.5 \text{ Nm}$  for V = 7 m/s and  $\lambda_d = 7$ .

$M_{hs \text{ tot}}$  is negative because the clockwise aerodynamic moment is defined positive. This is not logic for the description of the pitch movement. So from now on, the anti clockwise aerodynamic moment is defined positive and this results in a positive value of  $C_m$  and  $M_{hs \text{ tot}}$ . So  $M_{hs \text{ tot}} = 7.5 \text{ Nm}$  and  $M_{hs \text{ tot}}$  results in increase of the blade angle  $\beta$ .

$M_{hs \text{ tot}}$  at V = 7 m/s must be equal to the spring moment  $M_s$ . The spring is situated at the front side of the connecting strip and is supported by a supporting beam which is bolted to the small side of the connecting strip. A lever is connected to the blade shaft by means of an M12 bolt. The front part of the spring is connected to the lever by a threaded rod and a hinge. The lever has a length  $r_1$  which is about 85 mm = 0.085 m. The spring moment is about the product of the spring force  $F_s$  and  $r_1$ , so  $F_s$  is given by:

$$F_s = M_s / r_1 \quad (\text{N}) \quad (23)$$

Substitution of  $M_s = M_{hs \text{ tot}} = 7.5 \text{ Nm}$  and  $r_1 = 0.085 \text{ m}$  in formula 17 gives that  $F_s = 88 \text{ N}$ . The spring must be designed such that the spring force  $F_s$  increases only a little at increasing blade angle. So a weak spring is needed. This makes the pitch control system very sensible and this will sharply limit the maximum rotational speed. The determination of the spring geometry is out of the scope of this chapter. The spring drawn in figure 7 is only an artist impression.

#### 9.4 Determination of the friction moment for the Permaglide bearings

A rotor blade is loaded in the axial direction by a bending moment which is caused by the rotor thrust or by the gyroscopic moment. A rotor blade is also loaded by its own weight in the tangential direction but the influence of this load is neglected concerning the friction moment of the bearings as this moment becomes zero every time a blade is in the vertical position. As the head is turned on the wind by a double vane (see chapter 10), the head rotation is rather slow and the gyroscopic moment can therefore be neglected. The rotor thrust  $F_t$  is given by formula 4.12 of KD 35 which is copied as formula 24.

$$F_t = C_t * \frac{1}{2} \rho V^2 * \pi R^2 \quad (\text{N}) \quad (24)$$

Formula 24 gives the rotor thrust on the whole rotor. The rotor thrust on one blade of a rotor with two blades  $F_{t \text{ bl}}$  is half the value of the thrust on the whole rotor, so:

$$F_{t \text{ bl}} = 0.5 C_t * \frac{1}{2} \rho V^2 * \pi R^2 \quad (\text{N}) \quad (25)$$

The thrust coefficient for the VIRYA-5 rotor is about 0.7 if the rotor runs at  $\lambda_d = 7$ .  $F_{t \text{ bl}}$  is calculated for the same wind speed which was also used to calculate  $M_{hs \text{ tot}}$ , so  $V = 7$  m/s. Substitution of  $C_t = 0.7$ ,  $\rho = 1.2$  kg/m<sup>3</sup>,  $V = 7$  m/s and  $R = 2.5$  m in formula 25 gives that  $F_{t \text{ bl}} = 202$  N. The distribution of the thrust over the rotor blade has about the shape of a triangle with the highest value at the blade tip. A triangle load gives a bending moment  $M_b$  at the hart of the rotor which is the same as the moment of a point load at  $2/3 R$ . To facilitate the calculation, it is assumed that the real thrust distribution can be replaced by a point load at  $2/3 R$ , so at  $r_t = 1.667$  m.

The blade shaft is supported in two INA Permaglide bearings. It is expected that the distance in between bearing no1 and bearing no 2 is 0.32 m. The distance  $a$  in between  $r_t$  and bearing no 1 is 1.182 m. The distance  $b$  in between  $r_t$  and bearing no 2 is 1.502 m (see fig. 1).

The reaction force  $F_1$  at bearing no 1 can be calculated by taking the balance of moments around bearing no 2. This gives:

$$F_1 = F_{t \text{ bl}} * b / (b - a) \quad (\text{N}) \quad (26)$$

Substitution of  $F_{t \text{ bl}} = 202$  N,  $b = 1.502$  m and  $a = 1.182$  m in formula 26 gives  $F_1 = 948$  N.

The reaction force  $F_2$  on bearing no 2 is given by:

$$F_2 = F_1 - F_{t \text{ bl}} \quad (\text{N}) \quad (27)$$

Substitution of  $F_1 = 948$  N and  $F_{t \text{ bl}} = 202$  N in formula 27 gives  $F_2 = 746$  N. The direction of  $F_1$  is frontwards but the direction of  $F_2$  is backwards. The blade will bend backwards because of the thrust and this results in a counteracting moment due to the centrifugal force in the blade. This counteracting moment reduces the bending moment in the blade and therefore the forces  $F_1$  and  $F_2$  are also reduced somewhat. But this effect on  $F_1$  and  $F_2$  is neglected.

Both bearings have an inside diameter of 20 mm and a length of 20 mm, so the projected area  $A = 20 * 20 = 400$  mm<sup>2</sup>. A load of 948 N on bearing no 1 results in a thrust pressure of 2.37 N/mm<sup>2</sup> which is very low for a Permaglide bearing. A load of 746 N on bearing no 2 results in a thrust pressure of 1.87 N/mm<sup>2</sup> which is also very low.

The friction coefficient  $\mu$  of Permaglide bearings depends on the thrust pressure (it increases at decreasing thrust pressure) and it is about 0.13 for the calculated values.

The friction moment  $M_f$  for a bearing with an inside bearing radius  $r_b$  ( $r_b$  is halve the inside bearing diameter) is given by:

$$M_f = \mu * F * r_b \quad (\text{Nm}) \quad (28)$$

### Bearing no 1

Substitution of  $\mu = 0.13$ ,  $F = 948 \text{ N}$  and  $r_b = 10 \text{ mm} = 0.01 \text{ m}$  in formula 28 gives  $M_{f1} = 1.23 \text{ Nm}$ .

### Bearing no 2

Substitution of  $\mu = 0.13$ ,  $F = 746 \text{ N}$  and  $r_b = 10 \text{ mm} = 0.01 \text{ m}$  in formula 28 gives  $M_{f1} = 0.97 \text{ Nm}$ .

So the total friction moment of both bearings together  $M_{f \text{ tot}} = 1.23 + 0.97 = 2.2 \text{ Nm}$ .

The friction moment of the thrust ball bearing is neglected. So the total friction moment is rather large if compared to the aerodynamic moment  $M_{hs \text{ tot}} = 7.5 \text{ Nm}$  and so the pitch movement will have a some hysteresis. But in practice there will always be some vibration in the rotor and this vibration will reduce the hysteresis. So it is expected that INA Permaglide bearings can be used as rotor blade bearings. However, this calculation shows that the aerodynamic moment is rather small with respect to the moment of the bearing friction and so the functioning of the system is rather sensible to bearing friction. The components of the pitch control mechanism should be manufactured that accurately that no extra bearing friction is created because the shaft ends of the blade shaft and the bearing seats of the Permaglide bearings are not perfectly in line!

## 9.5 Checking of the load on the thrust ball bearings

A thrust ball bearing has an inner diameter of 20 mm, an outer diameter of 35 mm and a thickness of 10 mm. The bearing code is 51104. As the bearing isn't build in and protected against weather influences, one should use a stainless steel version. The maximum rotational angel is only  $20^\circ$  and the rotational speed will be very low so the strength of the bearing is checked for the static load factor  $C_0$ .  $C_0 = 16600 \text{ N}$  for this bearing.

The bearing will be loaded by the centrifugal force in the blade. Only the blade mass is taken into account. The mass of the blade shaft is neglected because it is lying on a small radius. The centrifugal force  $F_c$  will be calculated for the blade mass concentrated in the centre of gravity of the blade. The blade has a length  $L = 2.35 \text{ m}$  and so the radius of the centre of gravity  $r_c$  is given by:  $r_c = 2.5 - 0.5 * 2.35 = 1.325 \text{ m}$ . The blade is made out of hard wood with a density of about  $\rho_{bl} = 0.6 * 10^3 \text{ kg/m}^3$ . The cross sectional area  $A$  of the Gö 711 airfoil with a chord of  $c = 0.24 \text{ m}$  and a thickness  $t = 0.0357 \text{ m}$  is about given by  $A = 0.7 * c * t$  so  $A = 0.7 * 0.24 * 0.0357 = 0.006 \text{ m}^2$ . The blade mass  $m$  is given by  $m = \rho_{bl} * A * L$  so  $m = 0.6 * 10^3 * 0.006 * 2.35 = 8.46 \text{ kg}$ .  $F_c$  is given by:

$$F_c = m * r_c * \Omega^2 \quad (\text{N}) \quad (29)$$

The centrifugal force will be calculated for a rotational speed  $n = 187 \text{ rpm}$ , belonging to a frequency of 53 Hz and a wind speed of 7 m/s for the optimum cubic line (see figure 5).  $n = 178 \text{ rpm}$  gives that  $\Omega = \pi * 178 / 30 = 18.64 \text{ rad/s}$ . Substitution of  $m = 8.46 \text{ kg}$ ,  $r_c = 1.325 \text{ m}$  and  $\Omega = 18.65 \text{ rad/s}$  in formula 29 gives that  $F_c = 3899 \text{ N}$ . This is much lower than  $C_0 = 16600 \text{ N}$ , so the bearing is certainly strong enough.



### 9.6 Increase of $M_h$ by choosing the blade axis closer to the nose

In chapter 9.3 it was found that the total aerodynamic moment  $M_{hs\ tot}$  of the five blade sections  $M_{hs\ tot} = 7.5\ \text{Nm}$ . In chapter 9.4 it was found that the total friction moment  $M_{f\ tot} = 2.2\ \text{Nm}$ . So  $M_{f\ tot}$  is rather large with respect to  $M_{hs\ tot}$  and this will result in some hysteresis in the blade pitch movement.  $M_{f\ tot}$  can be reduced by taking needle bearings in stead of INA Permaglide bearings but these bearing are more sensible to the penetration of water and dust and they take more space. So this option isn't taken into account.  $M_{hs\ tot}$  can be increased by choosing of the blade axis closer to the airfoil nose. Assume that the blade axis is chosen at a distance of  $0.2 * c = 0.2 * 240 = 48\ \text{mm}$  from the nose. This results in increase of the value  $p$  and the angle  $\gamma$ . The new values of  $p$  and  $\gamma$  are illustrated in figure 8.

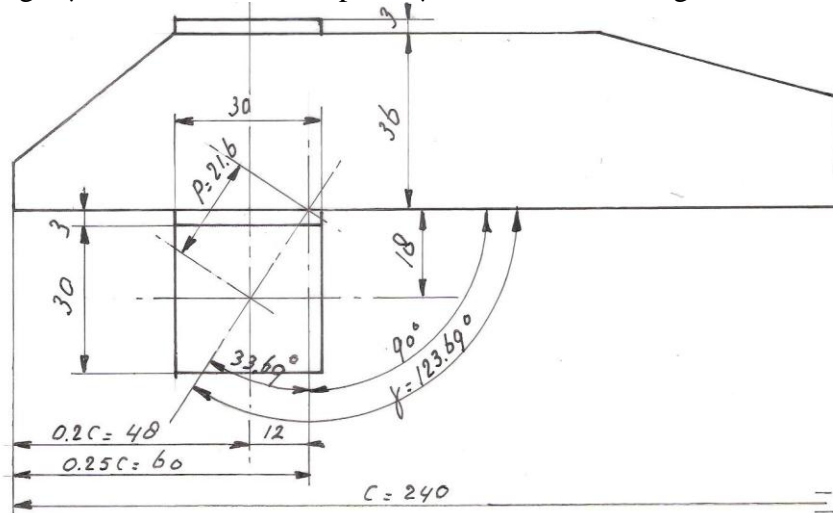


fig. 8 Change of  $p$  and  $\gamma$  for blade axis at  $0.2 * c$

Using figure 8 it can be calculated that  $p = 21.6\ \text{mm}$  and that  $\gamma = 123.7^\circ$ .  $p = 21.6\ \text{mm}$  and  $c = 240\ \text{mm}$  gives  $p / c = 0.09$ . Substitution of  $p / c = 0.09$  and  $\gamma = 123.7^\circ$  in formula 16 gives:

$$C_{mh} = C_{m0.25} + 0.09 \{C_l \cos(\alpha + 123.7^\circ) + C_d \sin(\alpha + 123.7^\circ)\} \quad (-) \quad (30)$$

Table 3 is now copied as table 5 but  $\alpha + 123.7^\circ$  is now used in stead of  $\alpha + 90^\circ$ .

$\alpha$ ( $^\circ$ )	$C_l$ (-)	$C_d$ (-)	$C_{m0.25}$ (-)	$\alpha + 123.7^\circ$ ( $^\circ$ )	$C_l \cos(\alpha + 123.7^\circ)$	$C_d \sin(\alpha + 123.7^\circ)$	$C_{mh}$ (-)
-14.1	-0.173	0.1640	-0.0174	109.6	0.0580	0.1545	0.0017
-11.6	-0.083	0.1275	-0.0350	112.1	0.0312	0.1181	-0.0216
-9.0	0.009	0.0928	-0.0554	114.7	-0.0038	0.0843	-0.0482
-6.2	0.070	0.0587	-0.0912	117.5	-0.0323	0.0521	-0.0894
-4.2	0.284	0.0299	-0.1236	119.5	-0.1398	0.0260	-0.1338
-2.2	0.483	0.0165	-0.1174	121.5	-0.2524	0.0141	-0.1388
0.0	0.665	0.0142	-0.1145	123.7	-0.3690	0.0118	-0.1466
2.1	0.843	0.0134	-0.1089	125.8	-0.4931	0.0109	-0.1523
4.3	1.019	0.0153	-0.1070	128.0	-0.6274	0.0121	-0.1624
6.6	1.190	0.0235	-0.1060	130.3	-0.7697	0.0179	-0.1737
8.8	1.361	0.0297	-0.1061	132.5	-0.9195	0.02190	-0.1858
11.3	1.479	0.0476	-0.1110	135.0	-1.0458	0.0337	-0.2021
14.3	1.478	0.1078	-0.1270	138.0	-1.0984	0.0721	-0.2194
17.8	1.354	0.2090	-0.1460	141.5	-1.0597	0.1301	-0.2297

table 5  $C_l$ ,  $C_d$ ,  $C_m$  and  $C_{mh}$  as a function of  $\alpha$  for  $Re = 4 * 10^5$  and for blade axis at  $0.2\ c$

$C_{mh}$  is now calculated for the new ratio  $p / c = 0.09$  and for the new angle  $\gamma = 123.7^\circ$ . The value of  $C_{mh}$  for this new blade axis at a distance of  $0.2 * c$  from the nose is now called  $C_{mh0.2}$ . Figure 6 of report KD 285 is now copied as figure 9. The calculated  $C_{mh0.2}-\alpha$  curve is added to figure 9.

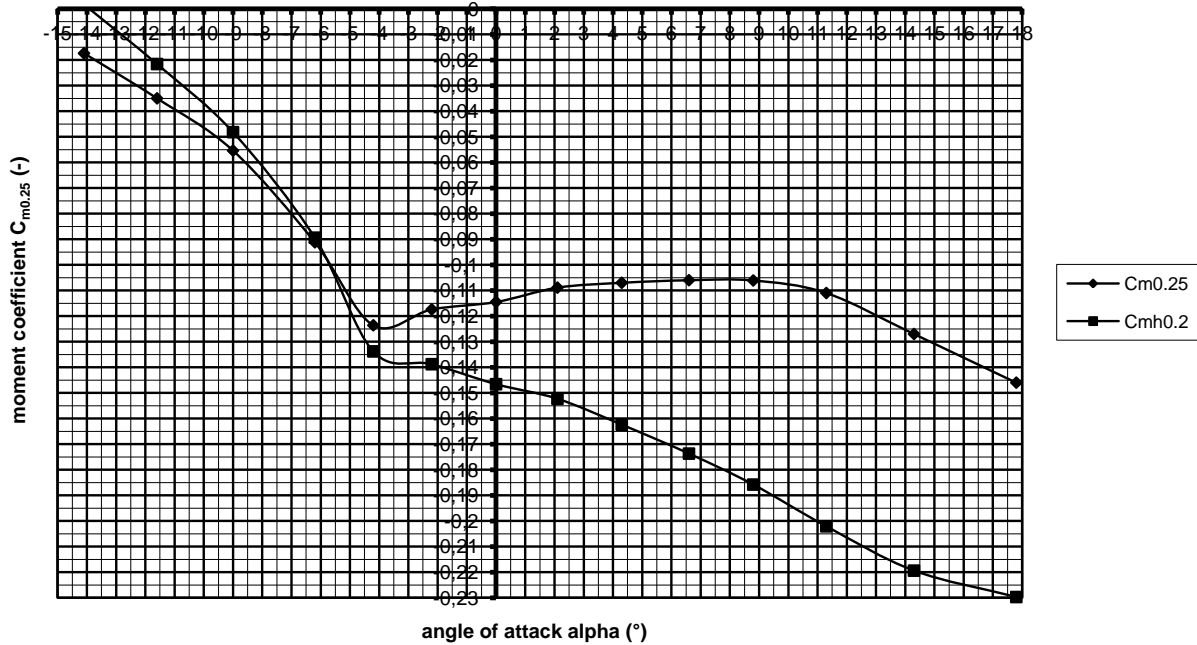


fig. 9  $C_{m0.25}-\alpha$  and  $C_{mh0.2}-\alpha$  curve for Gö 711 airfoil for  $Re = 4 * 10^5$

It can be seen that now there is a large difference in between both curves. The part of the curve which is relevant for the VIRYA-5 wind turbine is the part for values of  $\alpha$  about  $-2^\circ < \alpha$ . The  $C_{mh0.2}-\alpha$  curve decreases for  $-2^\circ < \alpha$ , so it is no longer allowed to make the calculations for a constant value of  $C_{mh}$  like it was done in chapter 9.3. Table 4 is now copied as table 6 but an extra column for  $\alpha_{lin}$  is added.  $\alpha_{lin}$  is copied from table 1 for the chosen sections. An extra column for  $C_{mh0.2}$  is added too. The value of  $C_{mh0.2}$  is read from figure 9 for the corresponding value of  $\alpha$ .

Section	r (m)	$\lambda_{rd}$ (-)	W (m/s) for V = 7 m/s	$\alpha_{lin}$ (°)	$C_{mh0.2}$ (-)	$M_{hs0.2}$ (Nm)
1	2.3	6.44	45.32	-0.1	-0.145	-4.110
2	1.9	5.32	37.53	1.1	-0.149	-2.865
3	1.5	4.2	29.77	2.9	-0.155	-1.896
4	1.1	3.08	22.06	6.0	-0.170	-1.142
5	0.7	1.96	14.49	12.0	-0.207	-0.600

table 6 r,  $\lambda_{rd}$ , W,  $\alpha_{lin}$ ,  $C_{mh0.2}$  and  $M_{hs0.2}$  as a function of the section number

Substitution of  $M_h = M_{hs0.2}$  ( $M_{hs0.2}$  is the contribution of a section),  $C_{mh} = C_{mh0.2}$ ,  $\rho = 1.2 \text{ kg/m}^3$ ,  $c = 0.24 \text{ m}$  and  $b = 0.4 \text{ m}$  in formula 18 gives:

$$M_{hs0.2} = C_{mh0.2} * 0.0138 * W^2 \quad (\text{Nm}) \quad (\text{for } V = 7 \text{ m/s}) \quad (31)$$

Next  $M_{hs0.2}$  is calculated for each section using formula 31. The total moment of all sections together is calculated by formula 22. This gives:

$$M_{hs0.2 \text{ tot}} = -4.110 - 2.865 - 1.896 - 1.142 - 0.600 = -10.613 \text{ Nm.}$$

The calculated value of  $M_{hs}$  for section 1 will be too high because of tip losses, so it is assumed that  $M_{hs \text{ tot}} = -10 \text{ Nm}$  for  $V = 7 \text{ m/s}$  and  $\lambda_d = 7$ .

$M_{hs0.2 \text{ tot}}$  is negative because the clockwise aerodynamic moment is defined positive. This is not logic for the description of the pitch movement. So the anti clockwise aerodynamic moment is now defined positive and this results in a positive value of  $C_{mh0.2}$  and  $M_{hs0.2 \text{ tot}}$ . So  $M_{hs0.2 \text{ tot}} = 10 \text{ Nm}$  and  $M_{hs0.2 \text{ tot}}$  results in increase of the blade angle  $\beta$ . So the total aerodynamic moment has increased from 7.5 Nm up to 10 Nm by shift of the blade axis from close to the quart chord point to a point lying at 0.2 c from the airfoil nose and the influence of the moment of the bearing friction therefore becomes less. Another advantage of this modification is that now the safety system will react more sensible to sudden wind gusts. A sudden wind gust means that the angel of attack  $\alpha$  increases suddenly for the whole blade and this results in increase of the pitch moment and so in increase of the blade angle  $\beta$  for wind speeds higher than 7 m/s. So this position of the blade axis is finally chosen.

$M_{hs0.2 \text{ tot}}$  at  $V = 7 \text{ m/s}$  must be equal to the spring moment  $M_s$ . The spring is situated at the front side of the connecting strip and is supported by a supporting beam which is bolted to the small side of the connecting strip. A lever is connected to the blade shaft by means of an M12 bolt. The front part of the spring is connected to the lever by a threaded rod and a hinge. The lever has a length  $r_l$  which is about  $85 \text{ mm} = 0.085 \text{ m}$ . The spring moment is given by: formula 23. Substitution of  $M_s = M_{hs \text{ tot}} = 10 \text{ Nm}$  and  $r_l = 0.085 \text{ m}$  in formula 17 gives that  $F_s = 118 \text{ N}$ . The spring must be designed such that the spring force  $F_s$  increases only a little at increasing blade angle. So a weak spring is needed. This makes the pitch control system very sensible and this will sharply limit the maximum rotational speed. The determination of the spring geometry is out of the scope of this chapter. The spring drawn in figure 7 is only an artist impression.

## 9.7 Determination of the compression spring geometry

In chapter 9.6 it has been determined that the compression spring must have a force  $F_s = 118 \text{ N}$  for a blade angle  $\beta = 6^\circ$ . The maximum blade angle  $\beta_{\text{max}} = 26^\circ$ . The displacement of the spring at the end of the threaded rod is about 30 mm for this angle. The increase of the spring force must be small for this displacement to make the system sensible enough to prevent too high rotational speeds. Assume that the spring force increases by a factor 5/4 so it becomes 147.5 N at  $\beta_{\text{max}} = 26^\circ$ . As the force increases linear to the displacement, this means that the total displacement  $s$  from the non compressed situation  $s = 5 * 30 = 150 \text{ mm}$ .

Assume that the outside diameter of the spring is 40 mm and that the spring is made out of stainless spring steel. Now the question is, what is the required non compressed length  $L$  and what is the required wire diameter  $d$  of such spring? The spring geometry is calculated using formulas given in chapter 9.1.1 of the blue (about 1990) catalogue of the Dutch spring manufacturer Hengelose Verenfabriek Bakker BV (ref. 8). There are two important formulas to calculate a compression spring.

$$F = s * G * d^4 / (8 * n * D^3) \quad (\text{N}) \quad (32)$$

$$\tau = 8 * F * D * k / (\pi * d^3) \quad (\text{N/mm}^2) \quad (33)$$

In these formulas  $F$  is the force (N),  $s$  is the displacement (mm) which belongs to  $F$ ,  $G$  is the shear modulus which is about  $80000 \text{ N/mm}^2$  for stainless steel,  $d$  is the wire thickness (mm),  $n$  is the active number of windings,  $D$  is the diameter of the spring at the heart line (mm),  $\tau$  is the torsional stress in the spring ( $\text{N/mm}^2$ ) and  $k$  is a correction factor which depends on the ratio  $d/D$ .

k is given in figure 2 of the catalogue but k is also given by the formula of Göhner which is:

$$k = 1 + 5/4 * d/D + 7/8 * (d/D)^2 + (d/D)^3 \quad (-) \quad (34)$$

Formula 33 gives the torsional stress at the heart line of the spring. However, the stress will be higher at the inside of the spring. How much higher depends on the ratio  $d/D$  and the increase of the stress is given by the factor k. Assume  $d = 3$  mm and  $D = 37$  mm. Substitution of  $d = 3$  mm and  $D = 37$  mm in formula 34 gives  $k = 1.108$ .

In formula 32 and 33 there are four unknowns  $d$ ,  $n$ ,  $D$  and  $\tau$  and only two knowns being  $F$  and the correspondent displacement  $s$ . To use the formulas, two other unknowns have to be estimated. This can be facilitated by using the nomograph given in figure 1 of the catalogue. This nomograph is given for different values of the ratio  $W = D / d$ . Assume  $D = 37$  mm and  $d = 3$  mm this gives  $W = D / d = 37 / 3 = 12.33$ . Assume take the column for  $W = 12$ . For a force of 147.5 N we read in figure 1 that  $d = 3$  mm. So  $d = 3$  mm for  $D = 37$  mm seems a good choice. The outside diameter of the spring is  $37 + 3 = 40$  mm and this corresponds to the spring which is designed in figure 7.

Next the active number of windings  $n$  has to be determined. Formula 32 can be written as:

$$n = s * G * d^4 / (8 * F * D^3) \quad (-) \quad (35)$$

Substitution of  $s = 150$  mm,  $G = 80000$  N/mm<sup>2</sup>,  $d = 3$  mm,  $F = 147.5$  N and  $D = 37$  mm in formula 35 gives  $n = 16.26$  rounded to 16.

The block length of the spring  $L_b$  is the spring length if all windings are compressed to each other.  $L_b$  depends on the spring ends. It is assumed that the spring wires are touching each other at the ends and that the ends are grind flat. The formula for  $L_b$  is given in figure 6 of the catalogue as:

$$L_b = 1.1 d (n + 1.5) \quad (\text{mm}) \quad (36)$$

Substitution of  $d = 3$  mm and  $n = 16$  in formula 36 gives  $L_b = 58$  mm.

The non compressed length of the spring  $L$  is the sum of the block length  $L_b$ , plus the minimum gap in between the windings which is 20 % of the total displacement, plus the total displacement  $s$ . So

$$L = L_b + 1.2 * s \quad (\text{mm}) \quad (37)$$

Substitution of  $L_b = 58$  mm and  $s = 150$  mm in formula 37 gives  $L = 238$  mm.

Next the torsional stress is calculated using formula 33. Substitution of  $F = 147.5$  N,  $D = 37$  mm,  $k = 1.108$  and  $d = 3$  mm in formula 33 gives  $\tau = 570$  N/mm<sup>2</sup>. In figure 3 of the catalogue, the allowable torsion stress is given depending on the material and the wire thickness. It can be read that the allowable stress is 800 N/mm<sup>2</sup> for stainless steel type X 12 Cr Ni 17 7 according to Din 17224 and for a wire thickness of 3 mm. So a stress of 570 N/mm<sup>2</sup> is allowed.

So the non compressed length of the spring  $L = 238$  mm. For a blade angle  $\beta = 6^\circ$ , the spring is compressed  $150 - 30 = 120$  mm. So the compressed spring length for  $\beta = 6^\circ$  should be drawn with a length of  $238 - 120 = 118$  mm in figure 7. The length of the treaded rod should be made that long that it is easy to tighten the spring. But probably it isn't necessary to make it that long that the spring can be tightened from the non compressed length.

## 9.8 Effect of braking the rotor on the safety system

The 34-pole PM-generator can be used as a brake by making short-circuit in the winding. As the generator has not yet been built and measured, the Q-n curve for short-circuit isn't known. So it isn't known at which rotational speed, the generator will have its peak torque. However, I have built and measured a 4-pole PM-generator using a housing frame size 132. The measurements for this generator are given in public report KD 82 (ref. 9). The Q-n curves for short-circuit in star and delta are given in figure 4 of this report. The Q-n curve for short-circuit in delta is lying highest because higher harmonic currents can circulate in the winding if the winding is connected in delta. It can be read that the maximum torque is about 115 Nm for a rotational speed of about 150 rpm. It isn't sure if a 34-pole generator of the same frame size has the same Q-n curve for short-circuit in delta. The peak torque might be about the same but the peak might lie at a higher rotational speed.

The rotor isn't stopped completely if short-circuit is made but it rotates at a very low rotational speed. This is because the  $C_q$ -value of the rotor at low values of  $\lambda$  is very low (see figure 3) and because the Q-n curve of the generator for short-circuit in delta is rising strongly for low rotational speeds. However, this rotational speed increases at increasing wind speed because the rotor torque increases quadratic with the wind speed (see formula 4.3 report KD 35). So there is always a certain very high wind speed for which the rotor torque becomes larger than the peak torque of the generator. So the rotor will accelerate if this wind speed is reached and a short-circuited generator can become very hot if it rotates short-circuited at a long time at high rotational speeds.

The situation is even worse if the rotor is provided with a positive pitch control safety system. There is a certain critical wind speed  $V_{crit}$  for which the blade angle  $\beta$  becomes bigger even if the rotor is running slowly. If this happens, the  $C_q$ -value of the rotor will increase strongly and this results in a sudden increase of the rotor torque which makes that the short-circuit torque of the generator is now certainly too low. The value of  $V_{crit}$  will now be determined.

The angle  $\phi$  is  $90^\circ$  for a non rotating rotor. The angle of attack  $\alpha$  is very large for a non rotating rotor. As the blade angle  $\beta = 6^\circ$  for the whole blade (see table 1), the angle of attack  $\alpha = 90^\circ - 6^\circ = 84^\circ$  (see KD 35 formula 5.2). If the rotor is rotating slowly, the angle  $\alpha$  will be smaller but it is still very large. The aerodynamic characteristics of the Gö 711 airfoil are only given up to an angle  $\alpha = 18^\circ$ . I have found only one airfoil for which the characteristics are given up to  $\alpha = 90^\circ$ . This is the NACA 4412 airfoil as measured by Imperial College. The  $C_l$ - $\alpha$  and  $C_l$ - $C_d$  curves are given at page 3-100 of report R 443 D (ref. 10). So it is not the  $C_d$ - $\alpha$  curve which is given but the  $C_l$ - $C_d$  curve. To find the  $C_d$ -value for a certain value of  $\alpha$ , one first has to read the  $C_l$ -value for this value of  $\alpha$  and then one can read the  $C_d$ -value at the x-axis for the same  $C_l$ -value. It can be read that the  $C_d$ -value is about 2 for  $75^\circ < \alpha < 90^\circ$ .

The  $C_m$ - $\alpha$  curve isn't given. However, the moment around the pitch axis is almost completely determined by the drag coefficient at very large values of  $\alpha$ . It is assumed that the drag  $D$  exerts at the middle of the chord, so at a distance  $0.5 c$  from the airfoil nose. It is also assumed that the pitch axis is lying at a distance  $0.2 c$  from the nose, so according to the situation as given in figure 8. So for the distance  $e$  in between the pitch axis and the point at which the drag exerts it is valid that  $e = 0.3 c$ . In chapter 9.6 it was calculated that the blade starts moving around the pitch axis at a moment of 10 Nm. The drag moment  $M_d$  is given by:

$$M_d = C_d * 0.5 \rho V_{crit}^2 * c * k * 0.3 c \quad (\text{Nm}) \quad (38)$$

Formula 38 can be written as

$$V_{crit} = \sqrt{(M_d / 0.15 * C_d * \rho * c^2 * k)} \quad (\text{m/s}^2) \quad (39)$$

Substitution of  $M_d = 10 \text{ Nm}$ ,  $C_d = 2$ ,  $\rho = 1.2 \text{ kg/m}^3$ ,  $c = 0.24 \text{ m}$  and  $k = 2 \text{ m}$  (see figure 1) in formula 39 gives that  $V_{\text{crit}} = 15.5 \text{ m/s}$ . This is a rather low wind speed and therefore stopping the rotor by making short-circuit is only allowed if no high wind speeds can be expected!

## 10 Description of the vane

The head must be turned into the wind. This yawing of the head around the tower axis causes a gyroscopic moment perpendicular to the plane of the rotor axis and the tower axis. The direction of the gyroscopic moment depends on the direction of rotation of the rotor shaft and of the direction of rotation of the head along the tower axis. The rotor turns always in the same direction but the yawing along the tower axis is half the time left hand and half the right hand. So the gyroscopic moment has half the time a tendency to push the rotor down and half the time to lift the rotor up. The gyroscopic moment in the blades and in the rotor shaft is maximal for the blades in vertical position and zero for the blades in horizontal position if the rotor has two blades. The gyroscopic moment is proportional to the angular velocity of the rotor, the angular velocity of the yaw movement and the moment of inertia of the rotor. So to limit the fluctuation of gyroscopic moment it is important that yawing takes place only slowly. The fluctuation of the gyroscopic moment is also reduced because the slender wooden blades are rather flexible.

A normal vane will turn the head too fast at high wind speeds. A system with side rotors which drive the head in the wind through a reducing gearing gives a very low yawing speed around the tower axis but this system is rather complicated and expensive. I have tested a so called double vane system on one of my earliest windmills, the DRIEKA-4, which had a rotor diameter of 4 m and a (very noisy) safety system with elastic air brakes on the blade tips. It was equipped with a 6 m long horizontal pipe parallel to the rotor plane with a square sheet on each end of the pipe. Each sheet makes an angle of  $20^\circ$  with the rotor axis and the direction of the angles is chosen such that touching lines along the sheets intersect with the rotor axis before the rotor. Each sheet had a width and height of 500 mm and was made of 4 mm steel sheet. A photo of the DRIEKA-4 is given in figure 10. It is expected that the same vane geometry can be used for the VIRYA-5.



fig. 10 The DRIEKA-4 windmill with double vane and tree tower designed in about 1985

The moment of inertia of this vane is very large and fast head movements are therefore damped very well. The optimum position of the pipe might be at the back side of the head frame just as it was also done for the DRIEKA-4. For this position, there is about balance of the vane weight and the weight of the generator and the rotor and this means that the moment on the yaw bearing housing is minimal.

## 11 References

- 1 Kragten A. Calculations executed for the 2-bladed rotor of the VIRYA-5 windmill ( $\lambda_d = 7$ , Gö 711 airfoil) meant for connection to a 34-pole PM-generator for driving the 1.1 kW asynchronous motor of a centrifugal pump. Description of the 34-pole generator. August 2016, modified November 2016, free public report KD 614, engineering office Kragten Design, Populierenlaan 51, 5492 SG Sint-Oedenrode, The Netherlands.
- 2 Kragten A. Ideas about a pitch control system for the VIRYA-15 windmill ( $\lambda_d = 8$ , Gö 711 airfoil, February 2010, free public report KD 437, engineering office Kragten Design, Populierenlaan 51, 5492 SG Sint-Oedenrode, The Netherlands.
- 3 Kragten A. Development of a tubular tower for the VIRYA-4.2 and the VIRYA-4.6B2 windmills, March 2015, reviewed November 2016, free public report KD 582, engineering office Kragten Design, Populierenlaan 51, 5492 SG Sint-Oedenrode, The Netherlands.
- 4 Kragten A. Rectification of 3-phase VIRYA windmill generators, May 2007, reviewed October 2014, free public report KD 340, engineering office Kragten Design, Populierenlaan 51, 5492 SG Sint-Oedenrode, The Netherlands.
- 5 Kragten A. The Gö 711 airfoil for use in windmill rotor blades, June 2006, revised February 2010, free public report KD 285, engineering office Kragten Design, Populierenlaan 51, 5492 SG Sint-Oedenrode, The Netherlands.
- 6 Kragten A. Rotor design and matching for horizontal axis wind turbines, July 1999, free public rapport KD 35, engineering office Kragten Design, Populierenlaan 51, 5492 SG Sint-Oedenrode, The Netherlands.
- 7 Kragten A. Determination of  $C_q$  for low values of  $\lambda$ . Deriving the  $C_p$ - $\lambda$  and  $C_q$ - $\lambda$  curves of the VIRYA-1.8D rotor, July 2002, free public rapport KD 97, engineering office Kragten Design, Populierenlaan 51, 5492 SG Sint-Oedenrode, The Netherlands.
- 8 Blue catalogue Hengelose Verenfabriek Bakker, date probably about 1990, Petroleumhavenstraat 14, P.O. box 50, 7550 AB Hengelo, the Netherlands, telephone 074 2555444.
- 9 Kragten A. Measurements performed on a generator with housing 5RN132M04V with a standard 400/690 V winding provided with a 4-pole armature with neodymium magnets, June 2001, free public report KD 82, engineering office Kragten Design, Populierenlaan 51, 5492 SG Sint-Oedenrode, The Netherlands.
- 10 Hageman A. Catalogue of Aerodynamic Characteristics of Airfoils in the Reynolds number range  $10^4 - 10^6$ , June 1980. Report R 443 D, (former) Wind Energy Group University of Technology Eindhoven, (no longer available but a scan of this report can be found on my website at the bottom of the menu KD-reports).